A new genus and species of frog from the Kem Kem (Morocco), the second neobatrachian from Cretaceous Africa (#71346)

First submission

Guidance from your Editor

Please submit by 21 Mar 2022 for the benefit of the authors (and your \$200 publishing discount).



Structure and Criteria

Please read the 'Structure and Criteria' page for general guidance.



Custom checks

Make sure you include the custom checks shown below, in your review.



Author notes

Have you read the author notes on the guidance page?



Raw data check

Review the raw data.



Image check

Check that figures and images have not been inappropriately manipulated.

Privacy reminder: If uploading an annotated PDF, remove identifiable information to remain anonymous.

Files

Download and review all files from the <u>materials page</u>.

- 9 Figure file(s)
- 1 Table file(s)
- 1 Raw data file(s)
- 1 Other file(s)



New species checks

- ! Have you checked our <u>new species policies</u>?
- Do you agree that it is a new species?
- Is it correctly described e.g. meets ICZN standard?

Structure and Criteria



Structure your review

The review form is divided into 5 sections. Please consider these when composing your review:

- 1. BASIC REPORTING
- 2. EXPERIMENTAL DESIGN
- 3. VALIDITY OF THE FINDINGS
- 4. General comments
- 5. Confidential notes to the editor
- You can also annotate this PDF and upload it as part of your review

When ready submit online.

Editorial Criteria

Use these criteria points to structure your review. The full detailed editorial criteria is on your guidance page.

BASIC REPORTING

- Clear, unambiguous, professional English language used throughout.
- Intro & background to show context.
 Literature well referenced & relevant.
- Structure conforms to <u>PeerJ standards</u>, discipline norm, or improved for clarity.
- Figures are relevant, high quality, well labelled & described.
- Raw data supplied (see <u>PeerJ policy</u>).

EXPERIMENTAL DESIGN

- Original primary research within Scope of the journal.
- Research question well defined, relevant & meaningful. It is stated how the research fills an identified knowledge gap.
- Rigorous investigation performed to a high technical & ethical standard.
- Methods described with sufficient detail & information to replicate.

VALIDITY OF THE FINDINGS

- Impact and novelty not assessed.

 Meaningful replication encouraged where rationale & benefit to literature is clearly stated.
- All underlying data have been provided; they are robust, statistically sound, & controlled.



Conclusions are well stated, linked to original research question & limited to supporting results.

Standout reviewing tips



The best reviewers use these techniques

	n
	N

Support criticisms with evidence from the text or from other sources

Give specific suggestions on how to improve the manuscript

Comment on language and grammar issues

Organize by importance of the issues, and number your points

Please provide constructive criticism, and avoid personal opinions

Comment on strengths (as well as weaknesses) of the manuscript

Example

Smith et al (J of Methodology, 2005, V3, pp 123) have shown that the analysis you use in Lines 241-250 is not the most appropriate for this situation. Please explain why you used this method.

Your introduction needs more detail. I suggest that you improve the description at lines 57-86 to provide more justification for your study (specifically, you should expand upon the knowledge gap being filled).

The English language should be improved to ensure that an international audience can clearly understand your text. Some examples where the language could be improved include lines 23, 77, 121, 128 – the current phrasing makes comprehension difficult. I suggest you have a colleague who is proficient in English and familiar with the subject matter review your manuscript, or contact a professional editing service.

- 1. Your most important issue
- 2. The next most important item
- 3. ...
- 4. The least important points

I thank you for providing the raw data, however your supplemental files need more descriptive metadata identifiers to be useful to future readers. Although your results are compelling, the data analysis should be improved in the following ways: AA, BB, CC

I commend the authors for their extensive data set, compiled over many years of detailed fieldwork. In addition, the manuscript is clearly written in professional, unambiguous language. If there is a weakness, it is in the statistical analysis (as I have noted above) which should be improved upon before Acceptance.



A new genus and species of frog from the Kem Kem (Morocco), the second neobatrachian from Cretaceous Africa

Alfred Lemierre Corresp., 1, David C. Blackburn 2

Corresponding Author: Alfred Lemierre
Email address: alfred.lemierre@edu.mnhn.fr

Neobatrachia, a clade representing the majority of extant anuran diversity, is thought to have emerged and diversified during the Cretaceous. Most of early diversification of neobatrachians occurred in southern Gondwana, especially the regions that are today South America and Africa. Whereas five extinct neobatrachians have been described from the Cretaceous of South America in the last decade, only one is known from Africa. This difference in the known extinct diversity is linked to the lack of well-preserved specimens, understudy of fragmentary remains, and lack of known Cretaceous sites in Africa. Study of fragmentary anurans remains from Africa could allow for the identification of previously unknown neobatrachians, allowing for a better understanding of their early diversification. We reanalysed several previously described anuran specimens from the well-known Kem Kem beds, including using CT-scanning. Through our osteological study, we determined that several cranial bones and vertebrae represent a new hyperossified taxon, Cretadhefdaa taouzensis. Comparison to other hyperossified anurans revealed similarities and affinity with the neobatrachians Beelzebufo (extinct) and Ceratophrys (extant). Phylogenetic analyses supported this affinity, placing Cretadhefdaa within Neobatrachia in an unresolved clade of Ceratophryoidea. Cretadhefdaa is the oldest neobatrachian from Africa, and reveals that neobatrachians were already widespread throughout southern Gondwana during the earliest Late Cretaceous.

Départmenet Origine et Evolution, UMR 7207, Centre de recherche en Paléontologie, CNR/Sorbonne Université/MNHN, Museum national d'Histoire naturelle, Paris, France

² Department of Natural History, Florida Museum of Natural History, University of Florida, Gainesville, Florida, United States



1	A new genus and species of frog from the Kem Kem (Morocco), the second
2	neobatrachian from Cretaceous Africa
3	Alfred Lemierre ¹ , David C. Blackburn ²
4 5	1. CR2P- Centre de recherche en Paléontologie-CNRS/MNHN/Sorbonne Université, Paris, 75005, France
6 7	^{2.} Department of Natural History, Florida Museum of Natural History, University of Florida, Gainesville, FL 32611, USA
8	
9	
10	
11	
12	
13	
14	
15	
16	Corresponding Author:
17	Alfred Lemierre ¹
18	Email address: alfred.lemierre@edu.mnhn.fr



20

21

Abstract

22 Neobatrachia, a clade representing the majority of extant anuran diversity, is thought to have 23 emerged and diversified during the Cretaceous. Most of early diversification of neobatrachians 24 occurred in southern Gondwana, especially the regions that are today South America and 25 Africa. Whereas five extinct neobatrachians have been described from the Cretaceous of South 26 America in the last decade, only one is known from Africa. This difference in the known extinct 27 diversity is linked to the lack of well-preserved specimens, understudy of fragmentary remains, 28 and lack of known Cretaceous sites in Africa. Study of fragmentary anurans remains from Africa could allow for the identification of previously unknown neobatrachians, allowing for a better 29 understanding of their early diversification. We reanalysed several previously described anuran 30 31 specimens from the well-known Kem Kem beds, including using CT-scanning. Through our 32 osteological study, we determined that several cranial bones and vertebrae represent a new 33 hyperossified taxon, *Cretadhefdaa taouzensis*. Comparison to other hyperossified anurans revealed similarities and affinity with the neobatrachians Beelzebufo (extinct) and Ceratophrys 34 35 (extant). Phylogenetic analyses supported this affinity, placing Cretadhefdaa within Neobatrachia in an unresolved clade of Ceratophryoidea. Cretadhefdaa is the oldest 36 neobatrachian from Africa, and reveals that neobatrachians were already widespread 37 38 throughout southern Gondwana during the earliest Late Cretaceous.



40

41

42

Introduction

43	The Cretaceous is a key period in anuran evolution and diversification including the emergence
44	of major extant clades such as the Neobatrachia and Pipidae (Frazão et al., 2015; Feng et al.,
45	2017). The breakup of the Western Gondwana palaeocontinent during the Late Jurassic and
46	Early Cretaceous (McLoughlin, 2001; Blakey et al., 2008)—leading to the creation of the Central
47	and Southern Atlantic Oceans—may have contributed to the early diversification of the
48	Neobatrachia, just as it likely did for the Pipidae (Frazão et al., 2015; Feng et al., 2017). Several
49	neobatrachian taxa have been described in the last decade from the Cretaceous beds of South
50	America (Báez et al., 2009; 2012; Báez and Gómez, 2018; Agnolin et al., 2020), contributing to a
51	better understanding of early diversification of the Neobatrachia. Unfortunately, the fossil
52	record of Neobatrachia is scarce for the Cretaceous of Africa and includes only a single
53	described taxon: Beelzebufo ampinga from the Cretaceous of Madagascar (Evans et al., 2014).
54	However, the lack of both study and sampling is not limited to either African Cretaceous
55	outgroups or extinct Neobatrachia. In general, there are few well-preserved and identifiable
56	anuran fossils in Africa, with numerous sites yielding only few and fragmentary remains (e.g., de
57	Broin et al., 1974; Báez and Werner, 1996; Rage, 2008; Gardner and Rage, 2016) that are not
58	easily incorporated into phylogenetic analyses. This contrasts with South American



60

61

62

63

64

65

66

67

68

69

70

71

72

73

74

75

76

77

78

79

80

neobatrachians, several of which are known from well-preserved and mostly articulated specimens preserving much or all of the skeleton (Báez et al., 2012). In Africa, only a handful of sites contain enough fragmentary fossils referred to the same taxon to allow for comparisons to other frogs and inclusion in phylogenetic analyses (Evans et al., 2008, 2014). These few sites are critical to filling the gap in the fossil record of Neobatrachia and central to understanding their early diversification in Africa. The Kem Kem beds of Morocco (Cretaceous, 100 95 Ma; Ibrahim et al., 2020) are known for their rich terrestrial vertebrate fauna with numerous dinosaurs, fishes, sharks, turtles, and crocodiles (Zouhri, 2017). This fauna has been studied extensively in recent decades (Ibrahim et al., 2020) but there is only a single study of its amphibians. Rage and Dutheil (2008) provided evidence for three different anurans, including one pipid that they described as Oumtkoutia anae based on a neurocranium, as well as two indeterminate non-pipid anurans based on postcranial remains (Rage and Dutheil, 2008). They attributed several cranial fragments to an undescribed species (mainly based on relative size of the cranial and postcranial elements) with an ornamented and hyperossified skull, one of the earliest known from the Cretaceous of Africa. Agnolin (2012) later described a neobatrachian taxon (Calyptocephalellidae) from the Late Cretaceous of Argentina and reviewed several Gondwanan anurans with hyperossified skulls. In that study, he included the Kem Kem fossils which he referred to the Calyptocephalellidae based on cranial and postcranial characters. Because several subsequent studies (Báez and Gómez, 2018; Muzzopappa et al., 2020) highlighted anatomical and analytical errors in Agnolin (2012), the attribution of the Kem Kem fossils to the Calyptocephallelidae is questionable. Because Agnolin (2012) considered all of the "indeterminate" anuran remains



from the Kem Kem to be a single taxon in his study, several characters supporting the affiliation these fossils with the Neobatrachia are based on postcranial elements not clearly referable to the hyperossified cranial elements. Further, because Agnolin (2012) did not included the Kem Kem fossils in his phylogenetic analysis, their relationships were never formally tested.

Revaluation of the anatomy and phylogenetic affinities of this hyperossified Kem Kem frog may be important for deciphering the early diversification of neobatrachians during the Lower Late Cretaceous of Gondwana and filling a notable gap in the fossil record of African anurans.

Here, we use microcomputed tomographic scans (MicroCT scans) to provide new information about the anatomy of the hyperossified Kem Kem frog. These new data allow for a more complete anatomical study of this taxon, comparisons to other Cretaceous anurans, and a phylogenetic analysis to estimate its relationships. We describe this material as a new genus and discuss its importance for understanding neobatrachian diversification in Gondwana during the Cretaceous.

Geological Context

The specimens were collected in 1995 during an expedition organized by the University of Chicago and the Service géologique du Maroc at four different localities near Taouz and Oum Tkout (OT1c, TD1, TZ8a1 and TZ8a2 from Dutheil, 1999) from the Kem Kem beds (Ettachfini and Andreu, 2004; Cavin et al., 2010). The term "Kem Kem beds" (Sereno et al., 1996) refers to a large escarpment extending across southeastern Morocco, near the Morocco-Algerian border (Ibrahim et al., 2020: fig. 1A, C), with numerous exposures along its length. More recently,



103

104

105

106

107

108

109

110

111

112

113

114

115

116

117

118

119

120

these beds have been referred to as the Kem Kem group (Ibrahim et al., 2020), containing two formations: the Gara Sbaa and the Douira Formations. The anuran specimens discussed here were recovered from layers that can be correlated to the Douira Formation of the Kem Kem group (upper part of the Kem Kem; Ibrahim et al., 2020). The Douira Formation (as well as the Gara Sbaa Formation) has been correlated to the Bahariya Formation in Egypt (Sereno et al, 1996; Cavin et al., 2010), which is dated to the Early Cenomanian (Cavin et al., 2010). The Kem Kem group is topped by marine sediments correlated to the Cenomanian-Turonian transition (Cavin et al., 2010). Other analyses have confirmed the Cenomanian age (Ibrahim et al., 2020) and considered the Kem Kem group a single continuous deposit sequence from 100 to 95 Ma. The boundary between the Gara Sbaa and the Douira Formations is dated to 96 Ma and linked to the Mid-Cenomanian Event (Ibrahim et al., 2020). The Douira Formation—and the anuran specimens discussed here—are thus dated from the middle Cenomanian, approximately 96 to 95 Ma (Ibrahim et al., 2020). The Douira Formation contains strata that show a marine influence that increases over time. The deposits in the lower part of the formation, composed of sandstones and mudstones, are consistent with a river delta, whereas the deposits in the upper part, composed of interbedded mudstone with claystone, are characteristic of coastal and sabkha environments (see Ibrahim et al., 2020 for a complete description). There is no indication if the materials came from either lower or upper part of the Douria Formation.

121

122

Materials and Methods



124

Institutional Abbreviations

125	research collection, Chicago (USA)
126	The anuran fossils are curated in the vertebrate palaeontology research collection of the
127	University of Chicago. We generated MicroCT scans at the University of Florida's Nanoscale
128	Research Facility using a Phoenix v tome x M (GE Measurement & Control Solutions, Boston,
129	MA, USA). Voltage and current were customized for each specimen to balance resolution and
130	intensity contrast; scanning parameters are included in the metadata associated with the scans
131	on MorphoSource. The x-ray images were converted into tomogram slices using GE's
132	reconstruction software datos x (see Table S1 in Supplemental Data 1). Each stack of slices
133	produced was imported in the 3D reconstruction software Mimics 21.0 (Materialise, Leuven,
134	Belgium); before importation, slices were cropped to remove empty spaces. To further
135	decrease the data size, the slices were converted from 16 bits to 8 bits. The resulting slices have
136	an image resolution of 1580 \times 2144 pixels and a voxel size of 5.7 μm for the volume size. 3D
137	models were produced by segmenting each element using the 'thresholding' function (using the
138	contrast on greyscale images). 3D model of the endocast was produced by segmenting each
139	element using the "add" function. We used the same voxel resolution of 5.7 μm , with a
140	smoothing factor of 3 for one iteration, to homogenize the model resulting from the
141	segmentation. Data produced by segmentation were exported in the software 3matic 9.0 as
142	separate files (see Table S1 in Supplemental Data 1).

MNHN: Muséum National d'Histoire Naturelle, Paris (France); UCRC-PV: University of Chicago



The electronic version of this article in Portable Document Format (PDF) will represent a published work according to the International Commission on Zoological Nomenclature (ICZN), and hence the new names contained in the electronic version are effectively published under that Code from the electronic edition alone. This published work and the nomenclatural acts it contains have been registered in ZooBank, the online registration system for the ICZN. The ZooBank LSIDs (Life Science Identifiers) can be resolved and the associated information viewed through any standard web browser by appending the LSID to the prefix http://zoobank.org/. The LSID for this publication is: urn:lsid:zoobank.org:pub:DCACD333-53AA-4A6D-A0F0-9F9C180F0DD. The online version of this work is archived and available from the following digital repositories: PeerJ, PubMed Central SCIE and CLOCKSS.

Phylogenetic analyses

Our data matrix includes 88 taxa and 150 morphological characters (62 cranial and 75 postcranial characters, 12 from the hyobranchial apparatus, and one from soft-tissues) and is derived from that of Lemierre et al. (2021; see Appendix S1 3). We added two extinct hyperossified neobatrachian taxa (the new taxon described below from the Kem Kem, and *Hungarobatrachus szukacsi*) to test their affinities. *Hungarobatrachus szukacsi* Szentesi and Venczel, 2010 has recently been included into a reduced phylogenetical analysis (ref Venczel et al., 2021), and considered a neobatrachian. It is the oldest neobatrachian outside of Gondwana and essential to understand the diversification of the clade during the Cretaceous. These new taxa were scored from observation on 3D mesh files created for this study based on segmenting newly generated MicroCT scans (see above) and from literature (Szentesi and Venczel, 2010; Venczel et al., 2021).



166

167

168

169

170

171

172

173

174

175

176

177

178

179

180

181

182

183

184

185

All analyses were performed using TNT v.1.5 (Goloboff and Catalano, 2016). All analyses were conducted with cline (also called multi-state) characters ordered (characters 3, 9, 10, 14, 26, 34, 51, 52, 68, 93, 112, 121, 124, 125 and 126). Cline characters were ordered as several studies (Rineau et al., 2015, 2018) showed that analyses using ordered morphocline characters outperformed analyses using unordered characters, even when the ordering scheme is wrong (Rineau et al., 2018). Analyses consisted of heuristic searches with 1000 random addition sequences of taxa, followed by tree bisection reconnection (TBR) branch swapping, withholding 10 trees per repetition. The final trees were rooted using *Ascaphus truei* (Ascaphidae, Anura) and a strict consensus was created. Node supports were evaluated using Bremer support and standard nonparametric bootstrapping, with searches of 1000 replicates and collapsing groups below 5% frequency. Because the phylogeny resulting from above is strongly at odds with relationships inferred from those inferred with molecular genetic data, we performed an additional analysis using a constraint tree reflecting a consensus of recent molecular phylogenetic analyses. This included constraining the backbone of the tree to reflect early divergences in anuran evolution, as well as large-scale patterns of relationships within the two major clades of Neobatrachia (Hyloidea, Ranoidea). We did not constrain the placement of any extinct taxa and we also left relationships within major clades as polytomies so that relationships within them could be inferred by our morphological dataset. We based this constraint tree (available in the Supplemental Materials) primarily on recent phylogenomic analyses, including Feng et al (2017), Streicher et al. (2018), Yuan et al. (2018), and Hime et al. (2021).



186	Results
187	Systematic Paleontology
188	Anura Duméril, 1804
189	NEOBATRACHIA Reig, 1958
190	CRETADHEFDAA gen. nov.
191	
192	Type (and only known) species
193	Cretadhefdaa taouzensis sp. nov.
194	
195	CRETADHEFDAA TAOUZENSIS Sp. nov.
196	Holotype
197	UCRC-PV94, posterior braincase preserving incomplete frontoparietals, parasphenoid,
198	and prooticooccipitals.
199	Type locality
200	TD1, near the city of Taouz in southeastern Morocco (see Dutheil, 1999 for more information
201	on Kem Kem localities).
202	Stratigraphic range
203	Middle Cenomanian (96–95 Ma).



204	Referred materials
205	One incomplete squamosal from TD1 (UCRC-PV95); one incomplete maxilla from Tz8a1 (UCRC-
206	PV96); three incomplete presacral vertebrae, two from TD1 (UCRC-PV97–98) and one from
207	Tz8a1 (UCRC-PV101); one incomplete sacral vertebra from OT1c (UCRC-PV103).
208	Etymology
209	The genus nomen Cretadhefdaa is a combination of the word Cretaceous and a transliteration
210	of the pronunciation of the Arabic word ضفدع or <i>dhefdaa</i> (also sometimes written as <i>dheftha</i> or
211	thedfaa), meaning "frog." The specific epithet taouzensis recognizes the type locality, Taouz.
212	Diagnosis
213	A neobatrachian anuran with a hyperossified skull differing from all other anurans by the
214	following unique combination of characters: frontoparietals coossified, lacking a midline suture,
215	and covered in ornamentation of pits and ridges; frontoparietals bearing a smooth occipital
216	flange; no incrassatio frontoparietalis on the ventral surface of the frontoparietals; presence of
217	a deep, groove-like central recess on the posterodorsal surface of the braincase to each side of
218	the foramen magnum, and housing the foramen for the occipital artery. Diagnosis for the
219	species is same as for the genus.
220	
221	Description of the holotype (UCRC-PV94)
222	Osteological description



225

226

227

228

229

230

231

232

233

234

235

236

238

239

240

241

242

243

224 co-ossified and the sutures between the prooticooccipitals and frontoparietals are difficult to discern (Fig. 1A-G). The posterior portion of the frontoparietals is preserved. The two frontoparietals are coossified to one another, and no suture is visible on the frontoparietal table (Fig. 1A). The frontoparietal table is large and covered in an ornamentation of pits and ridges. The posterior margin of the frontoparietals is flanked by a large occipital flange that lacks ornamentation (Fig. 1A). The processes paraoccipitalis are reduced and fused to the underlying epiotic eminence (prominentia circularis ducti of Roček and Lamaud, 1995), and the posterior process is not distinct (Fig. 1A). There is no pineal foramen visible. In lateral view, the preserved portion of the pars contacta is a straight vertical lamina (Fig. 1B). Because the lateral expansion of the frontoparietal is broken along its entire length, its full extent is unknown. In ventral view, the frontoparietal table extends lateral to the pars contacta into a tectum supraorbitale, but its full extent is unknown because it is broken (Fig. 1A, B). There is no visible frontoparietal 237 incrassation on the ventral surface of the frontoparietals. In posterior view, the boundary between the frontoparietals and prooticoccipital bears a series of deep recesses (Fig. 1D, E). The recesses are located between the tall epiotic eminence and the posterior margin of the frontoparietal table and appear to form a single large, deep groove on each side of the braincase. However, three different recesses can be distinguished within each groove (medial, central, and lateral recesses in Fig.1E) that are each separated by well-defined ridges. Both the lateral and medial recesses are shallow, whereas the central recess is deep and houses a large,

UCRC-PV94 is the preserved posterior region of the braincase of Cretadhefdaa. All bones are



245

246

247

248

249

250

251

252

253

254

255

256

257

258

259

260

261

262

263

264

265

circular foramen for the occipital artery. The exit foramen for the occipital artery is visible on each lateral surface of the frontoparietal, ventral to the lateral extension of the table (Fig. 1B). The posterior region of the parasphenoid is preserved. The cultriform process is broken, preserving only its base. The alae are large and cover the ventral surface of the otic capsules. In ventral view, the alae bear a median keel on its surface, extending from its lateral margin to and slightly curving towards the posterior process of the bone (Fig. 1C). The posterior process is divided into two well-separated small extensions, oriented posterolaterally. These expansions are fused to the base of the occipital condyles (Fig. 1C). The prootic and exoccipital are coossified into a single prooticooccipital complex without a visible suture. Each prooticooccipital is co-ossified to the other along their medial margins, as well as to the frontoparietals (dorsally) and parasphenoid (ventrally). In dorsal view, the epiotic eminence is large, forming a broad lamina (Fig. 1A, D). The dorsal surface of the prootic is smooth. The crista parotica is not fully preserved, but likely extended laterally. There is no trace of an articulation facet with the squamosal on the preserved portion of the prooticoccipital (Fig. 1A). In anterolateral view, a large prootic foramen is present on the anterior surface of the prooticoccipital (Fig. 1B, F), and is fully enclosed in bone. In lateral view, anterior to the prootic foramen, a notch is visible on the anteriormost bony margin of the braincase (Fig. 1B) and might represent the posterior portion of the optic foramen. In anterior view, a well-delimited, narrow groove, likely for the jugular vein, extends from a large depression at the border of the prootic foramen to the lateral margin of the prootic (Fig. 1F). Beneath this groove, a large depression is present from the lateral margin of the prootic to the midpoint of its anterior surface. This is likely an articular facet for the medial ramus of the pterygoid. In posterior view,



the left occipital condyle is missing (Fig. 1D), but the right occipital condyle is slightly ventrolateral to the large foramen magnum (Fig. 1D). The occipital condyle obscures the jugular foramen that remains partially visible laterally (Fig. 1D). In medial view, several foramina are visible in the wall of the braincase. The posteriormost opening is the jugular foramen (Fig. 1G). Separated from the latter foramen by a thin bony pillar, a large opening is present on the lateral braincase wall (Fig. 1G). This opening likely represents the fused acoustics foramina. This fusion might be the result of damage during the preservation, or by the absence of a bony separation between the two foramina. A similar preservation is also present in the exceptionally preserved *Thaumastosaurus servatus* Filhol 1877 (Lemierre et al., 2021).

Inner Ear

The preservation of the otic capsule allowed us to segment the otic chamber and semi-circular canals (vestibular apparatus) of *Cretadhefdaa*. The anterior, posterior, and lateral canals are all preserved and clearly identifiable (Fig. 2A, B). In anterior view, the base of the anterior canal bears a bulge, containing the anterior ampulla (Fig. 2A). In dorsal view, at the base of both anterior and lateral canals, the bulges contain the anterior and lateral ampullae (Fig. 2C). At the base of the posterior sinus (connecting the lateral and posterior canals), a similar bulge contains the posterior ampulla (Fig. 2B, D). In anterior and posterior views, the superior sinus (common crus), connecting the anterior and posterior canals, is well preserved (Fig. 2A C). The base of the superior sinus is thick, and is part of the utricle. The utricle forms the ventral portion of the vestibular apparatus. The vestibular apparatus occupies approximately half of total height of the endocast. The auditory region is large and bulbous (Fig. 2), and the perilymphatic cistern



289

290

291

292

293

294

295

296

297

298

299

300

301

302

303

304

305

306

307

308

from the rest of the ventral volume by a slight constriction (Fig. 2A, B). This region can be identified as the lateral chamber (Wever, 1979). The posterolateral surface of the lateral chamber bears a flattened surface, that corresponds to the oval window, where the footplate of the columella (and the operculum if present) would have abutted the inner ear (Wever, 1985; Maddin et al., 2013). In the posteromedial region of the perilymphatic cistern, a short and large canal, representing the perilymphatic duct, opens posteriorly (Fig. 2B, D) into the braincase and the condyloid fossa (i.e., "round window"; Wever, 1985). Another large duct is visible in the medial region of the otic chamber, entering the braincase through the fused acoustic foramina. However, this canal comprises two smaller ducts that are fused medially (Fig. 2) and housed the pathway of the cranial nerve VIII (Gaupp, 1896), representing the acoustic nerve (Duellman and Trueb, 1994). This confirms that the large foramina of the medial wall of the braincase is the fusion of the two acoustic foramina of Cretadhefdaa. A second medial, smaller duct is visible in the medial region of the vestibular apparatus, leading to the dorsalmost foramen of the medial wall of the braincase (Fig 1G). This duct is identified as the endolymphatic duct, leading to the endolymphatic sac that was present in the braincase (Frishkof and Goldstein, 1963; Duellman and Trueb, 1994).

Referred Cranial Material

UCRC-PV95

The specimen is a fragment of a right squamosal preserving a part of the otic plate (ramus paroticus) and the posterior process. The dorsal and lateral surface of the bone is covered with an ornamentation made of deep longitudinal pits and ridges in the anterior and temporal



310

311

312

313

314

315

316

317

318

319

320

321

322

323

324

325

326

327

328

329

region, and deep, nearly circular pits and ridges in the posterior and otic region. This ornamentation is slightly different from that observed in UCRC-PV94, though it is not uncommon for anuran cranial bones to display variation in ornamentation within an individual (Buffrénil et al., 2015, 2016). Thus, we interpret UCRC-PV95 as belonging to the same taxon as UCRC-PV94. The size of the squamosal is consistent with the size of the braincase (UCRC-PV94), but there is no indication that the two bones belong to the same individual. The otic plate is well developed (~3 mm length, anterior to posterior) and bears a vertical lamina on its ventral surface near the medial margin of the plate. On this lamina, a small ventral ridge is present, and delimits several ventral recesses. This system of ventral ridge and recesses resembles the one recovered in Beelzebufo ampinga (Fig. 3; Evans et al., 2014: fig. 18). In Beelzebufo, this system has been interpreted as an interlocking joint for the lateral end of the crista parotica (Evans et al., 2014). A similar interpretation can be made for Cretadhefdaa. This indicates that the squamosal extended medially and contacted the frontoparietals. However, we cannot be certain whether the squamosal covered the entire dorsal surface of the otic capsule (as in Beelzebufo) or if a supratemporal fenestra was present.

The posterior process is thick and elongate mediolaterally. Its medial surface is concave towards its center and forms a shallow recess near the junction of the posterior process and the otic plate. The posterior margin lacks ornamentation and bears a shallow depression on its ventral surface. The ventral margin of the posterior process is straight. The shallow depression was likely an articular facet for the quadratojugal (Fig. 3).

UCRC-PV96



This represents the middle portion of a left maxilla. The maxilla is toothed and its lateral surface is covered in a pits and ridges ornamentation. The ornamentation covers almost all of the lateral surface, save for a thin strip of bone ventrally and its dorsalmost portion. Dorsally, the base of a large process is preserved. It likely served as an articular facet with the squamosal. In medial view, the pars dentalis is straight, with a small sulcus dentalis (visible in ventral view). The lamina horizontalis is faint, almost non-distinct from the medial surface of the maxilla. It forms a small ridge, with a shallow dorsal groove for the palatoquadrate. A deep maxillary recess is present medially. A groove for maxillary nerves extends dorsally from the maxillary recess to the dorsal part of the maxilla. This groove delimits a small articular facet oriented dorsomedially. It could be a facet for articulation with the palatine (neopalatine of Trueb, 1973). Because only the bases of several teeth are preserved, nothing can be said of the tooth morphology of *Cretadhefdaa*.

Referred Vertebrae

The four vertebrae attributed to *Cretadhefdaa* all have an anterior cotyle and a posterior condyle, indicating a procoelous condition of the vertebral column. Although the shape of the centrum varies among these specimens (UCRC-PV97, UCRC-PV101 and UCRC-PV103 are shorter than UCRC-PV98), their similar size and the shape of articular facets and zygapophyses suggests that they all represent the same taxon. In addition, the two best preserved vertebrae, UCRC-PV101 and UCRC-PV98, each has a similarly shaped low and short neural spine that is oriented posteriorly. In other anurans, there is documented variation in the length of the centra of



presacral vertebrae throughout the vertebral column (Evans et al., 2014; Lemierre et al., 2021: fig. 9). We attribute the above cranial elements and these vertebrae to *Cretadhefdaa* because they all represent non-pipid individuals of similar body size (following Rage and Dutheil, 2008).

UCRC-PV97

This specimen is a centrum of a procoelous vertebra, with the neural walls not preserved (Fig. 4A–C). The centrum is longer than wide (Fig. 4A, B). The posterior condyle is large and wide.

UCRC-PV98

This presacral vertebra is better preserved than UCRC-PV97, with most of the transverse process, one postzygapophysis, and the distal end of the neural spine missing (Fig. 4D–I). The width of the posterior condyle is the same as that of the vertebral canal. The neural walls are thick, with the base of the transverse processes protruding laterally. In dorsal view, the remnants of the transverse processes are subcylindrical and oriented posteriorly. Each prezygapophysis bears a large flat and ovoid-shaped articular facet that is oriented dorsomedially (Fig. 4F). The medial margin of this articular facet is a sharp, straight lamina constituting the medial end of the dorsal wall of the anterior vertebral canal. The neural spine is low and was likely short, though it is broken distally. The postzygapophysis is long, with an ovoid and flattened articular surface that is oriented ventrally (Fig. 4F). A small posterior lamina connects the neural spine and the medial margin of the postzygapophysis. The centrum is more elongate than UCRC-PV97 (Fig. 4G). In ventral view, the centrum is compressed lateromedially at midlength, giving the ventral surface an hourglass shape (Fig. 4G). In lateral view, a shallow depression with a blind foramen is visible at the midpoint of the vertebra and is likely a spinal



375

376

377

378

379

380

381

382

383

384

385

386

387

388

389

390

391

foramen (Fig. 4H, I). The elongate centrum indicates that this vertebra is from the mid-column of *Cretadhefdaa*, possibly representing presacral vertebra IV.

UCRC-PV101

This element is an incomplete presacral vertebra preserving the centrum and neural arch (Fig. 4J-N). The centrum is short, almost as wide as large. The vertebra is procoelous, with an anterior cotyle and a posterior condyle (Fig. 4J, K). The condyle is poorly preserved but seems elongate lateromedially. The prezygapophyses bear a flat articular facet that is oriented dorsomedially (Fig. 4L). In dorsal view, the anterior margin of the neural arch is concave posteriorly, and a sharp ridge is visible on the dorsal surface of the neural arch, marking the beginning of the neural spine. The neural spine is very short (shorter than the one recovered in UCRC-PV98) and oriented posteriorly. Each postzygapophysis bears a flat articular surface that is oriented ventrolaterally. The transverse processes are broken at their bases. The base of these processes is cylindrical in shape and elongate anteroposteriorly, oriented perpendicular to the anteroposterior axis of the centrum (Fig. 4L, N). The anteroposteriorly short centrum and the low and posteriorly oriented neural spine indicate that UCRC-PV101 is one of the posterior presacral vertebra (VI to VIII). The posterior condule of UCRC-PV101 is similar in size to the anterior cotyle of the identified sacral vertebra (UCRC-PV103) and the inferred position of the prezygapophyses of UCRC-PV103 seems to match the position of the postzygapophyses of UCRC-PV101. UCRC-PV101 might represent the last presacral vertebra (VIII).

UCRC-PV103



This incomplete sacral vertebra bears an anterior cotyle and two posterior condyles (Fig. 40–R). The centrum of UCRC-PV103 is shorter than the other three vertebrae, but the anterior cotyle is similar to those of UCRC-PV97–98 and 101. The two posterior condyles are well separated and are wider than tall, and thus elliptical. The preserved transverse process is posterolaterally oriented and the preserved portion does not expand distally. In lateral view, the sacral transverse process is extended anteroposteriorly, and is not cylindrical or rod-like. The dorsal expansion of the transverse process is visible in dorsal view (Fig. 4R).

Osteological comparison to hyperossified anurans

Hyperossified (sensu Trueb, 1973) ornamented cranial bones occur in both extinct and extant anurans, from pipoids (Báez and Rage, 1998; Trueb et al., 2000) to diverse lineages of neobatrachians, and has evolved more than 20 times independently across extant frogs (Paluh et al., 2020). Hyperossified cranial elements are known in numerous Cretaceous anurans from both Laurasian and Gondwanan sites (Jacobs et al., 1990; Rage and Roček, 2003; Roček, 2013; Gardner and Rage, 2016). In the Gondwanan fossil record, Cretaceous hyperossified anurans are known that belong to both the Pipimorpha and Neobatrachia (Gardner and Rage, 2016; Gómez and Báez, 2018).

Comparison to non-neobatrachian taxa

Ornamented and co-ossified cranial bones are relatively uncommon in the first four diverging lineages of extant frogs: Leiopelmatoidea, Alytoidea, Pipoidea, and Pelobatoidea. Neither of the two extant leiopelmatoids, *Ascaphus* and *Leiopelma*, exhibit any characteristics unique to hyperossified anuran skulls. Among the extant alytoids, ornamented dermal bones are found



414

415

416

417

418

419

420

421

422

423

424

425

426

427

428

429

430

431

432

433

434

only in the genus Latonia which is known from the Paleogene and Neogene of Laurasia and Africa (Roček, 1994; 2013; Biton et al., 2016). However, Cretadhefdaa differs from Latonia in having a foramen for the occipital artery (lacking in Latonia) and frontoparietals that coalesce and fuse with the prooticooccipitals (see Roček, 1994: fig. 7). The extinct Gobiatidae from the Cretaceous of Asia (Roček, 2008; 2013) also exhibits ornamented dermal bones. However, Cretadhefdaa can be differentiated from all Gobiatidae in having fused frontoparietals without a visible suture (frontoparietals not fused or in contact with each other in Gobiatidae), complete fusion of the prootic and exoccipital (suture visible between the two bones in Gobiatidae; Roček, 2008), and presacral vertebrae that are procoelous (amphicoelous in Gobiatidae). Cretadhefdaa can be differentiated from all pipoid anurans in having alae of the parasphenoid that cover the ventral surface of the otic capsules (Fig. 1C). Some members of the Pelobatoidae also have ornamented skull bones, but as an integral part of the bone and not as a secondary exostosis (Rage and Roček, 2007; Roček, 2013; Roček et al., 2014) as seen in Cretadhefdaa. In addition, several fragmentary remains of ornamented maxillae and procoelous vertebrae were recovered in the Cretaceous outcrops of Texas and might represent one the early diverging frog lineages, but the phylogenetic affinities of these fossils remain unclear (Roček, 2013). Based on these comparisons, we exclude Cretadhefdaa from the Leiopelmatoidea, Alytoidea, Pipoidea, and Pelobatoidea. The vast majority of extant frog species belong to the Neobatrachia. Cretadhefdaa shares with Neobatrachia the presence of well-separated occipital condyles and a bicondylar articulation between the sacrum and urostyle. However, the principal synapomorphies used to diagnose



- 435 Neobatrachia, such as the presence of palatines (also called neopalatines in neobatrachians;
- 436 Báez et al., 2009) cannot be assessed based on the preserved elements of *Cretadhefdaa*.

Comparison to Cretaceous hyperossified taxa

438 The best known non-pipimorph ornamented taxon described from the Mesozoic fossil record of 439 Africa is Beelzebufo ampinga Evans et al. 2008, from the Maastrichtian of Madagascar (Evans et al., 2008, 2014). Beelzebufo is known from numerous cranial and some postcranial elements. 440 The ornamentation of *Cretadhefdaa*, comprised of pits and ridges, is similar to that of 441 Beelzebufo. Both taxa also have a series of three recesses on the posterodorsal surface of the 442 443 braincase, with the foramen for the occipital arteria located within the central recess, which is 444 the deepest recess in both taxa (Fig. 5). Cretadhefdaa also differs from Beelzebufo in having a smooth occipital flange on the posterior region of the frontoparietals. The poor preservation of 445 the lateral expansion of the frontoparietals of Cretadhefdaa (UCRC-PV94) means that we 446 cannot evaluate whether it is similar to the expansion in Beelzebufo, in which the lateral 447 expansion is elongate laterally along on its entire length, covering the lateral region of the 448 449 braincase (Evans et al., 2014). The parasphenoid of Cretadhefdaa is similar to that of Beelzebufo in having narrow alae (alary process of Evans et al., 2014) with a median keel. Cretadhefdaa is 450 451 similar to Beelzebufo in lacking a distinct palatine shelf on the medial surface of the maxilla, but differs in having ornamentation of the pars facialis on the lateral surface of the maxilla that 452 extends ventrally to the pars dentalis (the ornamentation ends before the pars dentalis in 453 454 Beelzebufo).



456

457

458

459

460

461

462

463

464

465

466

467

468

469

470

471

472

473

474

475

476

The presacral vertebrae of Cretadhefdaa differ from most of those referred to Beelzebufo by lacking a well-developed neural spine that is both tall and thick as well as the expanded and ornamented "table" sitting atop the spine (Evans et al., 2014: fig. 34-36); even the shortest neural spine of the posteriormost presacral of Beelzebufo is taller than that of any vertebrae that we refer to Cretadhefdaa (Fig. 4F, L). The sacral vertebra of Cretadhefdaa is similar to that of Beelzebufo in having two elliptical posterior condyles for the sacro-urostylar articulation and a centrum that is wider than longer (Fig. 4P). However, the sacral transverse processes of Beelzebufo are slightly more expanded distally than that preserved for Cretadhefdaa (Fig. 4R). Another neobatrachian from Gondwana with an ornamented skull is Baurubatrachus pricei Báez and Perí, 1989 from the Crato Formation of Brazil (Upper Early Cretaceous). The poor preservation of the frontoparietals of the holotype (and only known specimen), which is still embedded in matrix, prevents comparisons of the braincase of Cretadhefdaa to Baurubatrachus. However, its frontoparietals seem similar in having ornamentation comprised of pits and ridges that extend posteriorly to the margin of the foramen magnum. Cretadhefdaa also differs from B. pricei in having a fully ossified dorsal margin of the foramen magnum, and an exit foramen for the occipital artery that is dorsal to the prootic foramen. The maxilla of Cretadhefdaa is similar to B. pricei in having ornamentation on the lateral surface of the pars facialis that extends ventrally to the pars dentalis, but differs in lacking a distinct palatine shelf. Cretadhefdaa differs from B. pricei in having an occipital flange and a system of recesses on the posterodorsal region of the braincase. Cretadhefdaa also differs from B. pricei in having more slender and shorter neural spines on presacral vertebrae and slightly expanded sacral transverse processes.



478

479

480

481

482

483

484

485

486

487

488

489

490

491

492

493

494

495

496

497

498

In his 2012 review, Agnolin described several specimens as Calyptocephalella satan, the oldest calyptocephalellid described (Agnolin, 2012). Although these specimens need to be reassessed (Báez and Gómez, 2018) and likely represent more than one taxon (Muzzopappa et al., 2020), their attribution to Calyptocephalellidae is certain. Cretadhefdaa resembles C. satan in having dermal skull bones covered with an ornamentation of pits and ridges, but differs in lacking a distinct palatine shelf (all calyptocephalellids exhibit a distinct palatine shelf; Muzzopappa and Báez, 2009; Agnolin, 2012), in having fused frontoparietals without a medial suture, and in having an occipital flange on the frontoparietals (Fig. 1A). The postcranial elements of Cretadhefdaa resemble C. satan in having procoelous vertebrae with anteroposteriorly elongate centra for the anterior presacral vertebrae, and shorter centra for posterior presacral and sacral vertebrae (Agnolin, 2012). The sacral vertebra bears a bicondylar articulation in both taxa, but Cretadhefdaa differs in having sacral transverse processes that are weakly expanded distally, whereas C. satan exhibits greatly expanded sacral transverse processes (Agnolin, 2012: fig. 10A, B). One last ornamented Cretaceous neobatrachian taxon is Hungarobatrachus szukacsi Szentesi & Venczel, 2010 from the Late Cretaceous of Hungary. Its vertebral elements are not known, but several skull fragments were recently described (Venzcel et al., 2021). Both taxa have fused frontoparietals without a trace of suture along their medial margin. However, Cretadhefdaa differs from H. szukacsi in having a system of recesses on each side of the posterior surface of its frontoparietals (divided by the posterior process) with the foramen for the occipital artery opening in a deep recess and an occipital flange on the frontoparietals. In H. szukacsi, the posterior surface of the frontoparietals is smooth with a slight depression and the foramen for



500

501

502

503

504

505

506

507

508

509

510

511

512

513

514

515

516

517

518

519

the occipital artery opens on each side of the posterior process (Venczel et al., 2021: fig.3). The frontoparietals of *H. szukacsi* also bear an incrassatio frontoparietalis on the ventral surface whereas *Cretadhefdaa* does not. The maxilla of *Cretadhefdaa* differs from that of *H. szukacsi* in lacking a distinct palatine shelf (Venczel et al., 2021: fig. 5).

Comparison to hyperossified extinct ranoids

Two other hyperossified taxa are relevant for comparisons to Cretadhefdaa: Rocekophryne ornata Rage et al. 2021 from the Early Eocene of Algeria (Rage et al., 2021) and Thaumastosaurus servatus Filhol 1877 from the Middle to Late Eocene of southwestern France (Lemierre et al., 2021). These are the oldest occurrences of ornamented ranoids in the fossil record (Lemierre et al., 2021; Rage et al., 2021). Rocekophryne ornata is known from fragmentary cranial and postcranial remains. Cretadhefdaa resembles Rocekophryne in having fused frontoparietals without a median suture and bearing an ornamentation of pits and ridges, an occipital flange, and in lacking an incrassatio frontoparietalis on the ventral surface of the frontoparietals. In addition, Cretadhefdaa and Rocekophryne both bear ornamentation on the lateral surface of the pars facialis of the maxilla that extends ventrally to the pars dentalis (Fig. 3F). However, Cretadhefdaa differs in lacking a lateral flange on the posterior surface of the frontoparietal, lacking a distinct palatine shelf, and in having very short processes paraoccipitalis (well-developed in Rocekophryne; Rage et al., 2021: fig. 3A—F) and a series of recesses on the posterodorsal surface of the braincase. In addition, the sacral vertebra of Rocekophryne bears an anterior condyle (instead of an anterior cotyle in Cretadhefdaa) that indicates that the vertebral column is diplasiocoelous (Rage et al.,



2021: fig. 4A, B) and possesses transverse processes that are circular in lateral view (not circular in *Cretadhefdaa*).

Thaumastosaurus servatus is known from fragmentary remains and three partially complete and articulated skeletons (Rage and Roček, 2007; Lemierre et al., 2021). As with *R. ornata*, *Cretadhefdaa* and *T. servatus* have fused and ornamented frontoparietals without a medial suture. The anterior surface of the prooticooccipitals of both taxa exhibit a well-delimited but shallow and narrow groove for the jugular vein (Rage and Roček, 2007: fig. 7; Lemierre et al., 2021: fig. 8F). However, *Cretadhefdaa differs* from *T. servatus* in having an occipital flange and reduced processes paraoccipitalis, lateromedially compressed occipital condyles (instead of crescent shaped), and a series of recesses in the posterodorsal surface of the braincase (Fig. 1). *Cretadhefdaa* also differs from *T. servatus* in lacking a single, tapered posterior process of the parasphenoid and an incrassatio frontoparietalis on the ventral surface of the frontoparietals (Fig. 1C). In addition, the vertebral column of *T. servatus* is diplasiocoelous instead of procoelous as in *Cretadhefdaa*.

Comparisons to extant hyperossified hyloids

Cretadhefdaa shares numerous characters with ornamented extant Neobatrachia. Most of these similarities are associated with hyperossification, but two characters deserve further attention. The first is the presence of contact between the squamosal and frontoparietals, which occurs frequently (but not uniquely) in Hyloides (e.g., Calyptocephalellidae, Ceratophryidae, or the hylid *Triprion*). The second is the series of recesses on the posterodorsal surface of the braincase in *Cretadhefdaa*. This is known only in *Beelzebufo* and in *Ceratophrys*



(Evans et al., 2014; Fig. 5B, C). However, both *Cretadhefdaa* and *Beelzebufo* differ from *Ceratophrys* in having the foramen for the occipital artery located in the central recess, whereas it is found in the medial recess in extant taxa (Fig. 5). The braincase of *Ceratophrys* is similar to *Cretadhefdaa* in having fused frontoparietals, no distinct posterior process, and barely distinct processes paraoccipitalis. *Cretadhefdaa* differs from *Ceratophrys* in having an occipital flange, a well-delimited groove for the jugular vein, and in lacking the expanded "table" atop the neural spine of presacral vertebrae. The extant *Triprion* and *Diaglena* differ from *Cretadhefdaa* in having a frontoparietal extending posteriorly up to the end of the epiotic eminence, covering it dorsally. *Triprion* also lacks the system of recesses on the posterodorsal surface of the braincase. *Diaglena* bears recesses on it posterodorsal region of the braincase, but differs from *Cretadhefdaa* in having the foramen for the occipital artery not located within a recess.

- NEOBATRACHIA? Reig, 1958
- 554 RANOIDES? Frost et al., 2006

555 Forelimb (UCRC-PV104)

This specimen is an incomplete humerus missing it proximal end and part of the diaphysis (Fig. 6). The diaphysis is straight, and a thin ventral ridge on the proximal end of the bone extends distally to the midlength of the diaphysis (Fig. 6A, C). The fossa cubitalis is very reduced, being shallow and not well-delimited, and visible in ventral view only as a thin crescent around the humeral head (Fig. 6A). The humeral head is large and in-line with the main axis of the diaphysis. The epicondyles are not symmetrical, with the ulnar epicondyle well-developed and



563

564

565

566

567

568

569

570

571

572

573

574

575

576

577

578

579

580

581

the radial epicondyle reduced and barely visible in ventral view (Fig. 6A). In dorsal view, the olecranon scar is short, with a tapered and pointed end (Fig. 6B).

Comparisons

The combination of a large humeral head and asymmetrically developed epicondyles is diagnostic for most Neobatrachia (Prasad and Rage, 2004; Rage et al., 2013), although this combination of characters has not been evaluated in phylogenetic analyses. The presence of a straight diaphysis, a humeral head in line with the axis of the diaphysis, and a shallow, poorly delimited fossa cubitalis are found in most ranoids (Rage et al., 2013; de Lapparent de Broin et al., 2020). It differs from the humerus of *Thaumastosaurus servatus* Filhol, 1877, one of the earliest known ranoids, in having a crescent-shaped fossa cubitalis (triangular in *T. servatus*) and a less developed ulnare epicondyle. Among the Cretaceous neobatrachian taxa, only Eurycephalella alcinae Báez et al. 2009 and Arariphrynus placidoi Leal and Brito 2006 have preserved humeri with their ventral surface exposed. The humerus of A. placidoi differs from UCRC-PV104 in having two well-developed epicondyles (instead of a reduced radial epicondyle) and a deep fossa cubitalis (instead of a shallow fossa in UCRC-PV104). These comparisons suggest that UCRC-PV104 should be referred to the Neobatrachia. UCRC-PV104 shares several characters with extant and extinct Ranoides, as well as with the oldest (putative) member of the Ranoides (Thaumastosaurus servatus). However, because no phylogenetic analyses have yet shown synapomorphies for Ranoides related to the humerus, we refer this fossil to the Neobatrachia and recognize the assignment to Ranoides as tentative.

582



INCERTAE SEDIS

Pelvic girdle (UCRC-PV105)

This element is an incomplete left ilium, preserving most of its acetabular region. UCRC-PV105 bears a high and well-developed dorsal crest, although its extension on the ilial shaft is unknown (Fig. 7I J). The dorsal crest appears to be lacking its dorsalmost portion, indicating that it was more extensive (Fig. 7I, K). The dorsal prominence is low and elongate anteroposteriorly, and the dorsal protuberance is strongly oriented laterally (Fig. 7K). The acetabular rim is well developed on its ventral region. Although not complete, both the dorsal and ventral acetabular expansions are developed. The dorsal acetabular expansion is inclined posteromedially (Fig. 7I). Although poorly preserved, the ventral acetabular expansion was well-developed, extending ventrally (Fig. 4I). The preacetabular angle is obtuse and the preacetabular zone is narrow (Fig. 7I). In medial view, a shallow but well delimited medial ridge is present, starting from the base or the dorsal acetabular expansion to the anteriormost preserved portion (Fig. 7J). In posterior view, the ilioischiatic juncture is moderately wide and an interiliac tubercle is absent (Fig. 7L).

Comparisons

Ilia are one of the most common anuran elements recovered in the fossil record (Roček, 2000; Rage and Roček, 2003; Roček, 2013; Gardner and Rage, 2016) and several authors have proposed characters to identify the ilia of the different clades (Gardner et al., 2010; Gómez and Turazzini, 2016; Matthews et al., 2019). However, these are largely based on extant anurans and can be difficult to apply to Mesozoic anurans (Roček et al., 2010; Roček, 2013). The



presence of a well-developed dorsal crest is found in several clades (Alytoidea, Pipoidea, and Neobatrachia, especially Ranoides), but likely reflects similarity in locomotion rather than close phylogenetic relationships (Roček, 2013). The absence of an interiliac tubercle is diagnostic for many neobatrachians, with notable exceptions such as *H. szukacsi* and the aquatic hylid *Pseudis* (Gómez and Turazzini, 2016; Venczel et al., 2021). However, the utility of this character has not been tested thoroughly in a taxon-rich phylogenetic analysis (Gómez and Turazzini, 2016). Agnolin (2012) argued that the presence of a broad preacetabular zone and large acetabular fossa was diagnostic for the Calyptocephalellidae but this was not evaluated in a phylogenetic analysis and may represent an example of convergent evolution. There are no characters that allow for a precise attribution of this ilium (UCRC-PV105) to the other anurans from the Kem Kem or other specific anuran lineages.

Phylogenetic Analyses

Recent phylogenetic analyses (Báez and Gómez, 2018; Lemierre et al., 2021) are based on a similar dataset. This dataset was first elaborated by Báez et al. (2009), based on the dataset of Fabrezi (2006) that was developed for a phylogenetic analysis of ceratophryids. The dataset from Báez et al. (2009) includes 42 taxa—three of which are extinct taxa—and 75 characters. In a separate analysis, Báez and Gómez (2018) modified the dataset from Fabrezi (2006) further by adding 29 neobatrachian taxa and redefining some characters to test the impact of characters related to hyperossification. They expanded the taxon sampling to 71 taxa and added 68 characters (for a total of 143 characters), as well as redefined several characters.



Finally, Lemierre et al. (2021) further enlarged the dataset from Báez and Gomez (2018), by adding 15 extant natatanuran ranoid taxa (for a total of 20 natatanuran taxa). The vast majority of extant anurans belong to the Neobatrachia (Feng et al., 2017), which includes two large clades, the Hyloides and the Ranoides. To date, phylogenetic analyses based solely on morphological characters (e.g., Scott, 2005) do not recover many of the clades found in recent molecular phylogenetic analyses (e.g., Roelants et al. 2007; Feng et al., 2017; Jetz and Pyron, 2018; Hime et al. 2021). To evaluate the phylogenetic placement of *Cretadhefdaa*, we analyzed our character matrix using different sets of assumptions as well as one analysis using a constraint tree reflecting recent results from molecular phylogenetic analyses.

Results

We obtained 60 MPTs (most parsimonious trees) of 1362 steps (CI = 0.139; RI = 0.418) with the analysis performed under equal weight with cline characters ordered. The strict consensus (Fig. 7) shows large polytomies, and the monophyly of the Neobatrachia is not recovered. This seems to be linked to the uncertainties regarding the position of *Arariphrynus placidoi*, and the lack of characters scored for *Cretadhefdaa* and *Hungarobatrachus szukacsi* (13 and 11% of characters scored, respectively). *Cretadhefdaa* is recovered within a clade containing *Uberabatrachus* and the Ceratophryoidea. This clade is supported by three synapomorphies, all of which are character states found in other groups of frogs: (1) a position of articulation of lower jaw and skull at the level of occiput (character 61: 0 >1); (2) cotyle of the atlas widely separated (76: 1 >2) and (3) angle between iliac shaft and ventral acetabular expansion obtuse (125: 1 >2). *Cretadhefdaa* is placed within this clade in a polytomy with the Ceratophryidae.





647 characters (see Appendix S4 in Supplemental Data 1). 648 When excluding Arariphrynus, we obtained 10 trees of 1355 steps. The strict consensus (CI = 649 0.174; RI = 0.556; Fig. 8) shows a trichotomy with Pelobatoidae, Heleophryne, and the remaining Neobatrachia. The 'Neobatrachia' (the clade exclusive of Heleophryne) is supported 650 by a five synapomorphies: (1) otic plate of the squamosal short, overlapping only the most 651 lateral portion of the crista parotica (9: 0 >1); (2) absence of process or crest on the anterior 652 margin of the scapula (114: 3 >0); (3) configuration of the postaxial carpals as ulnare free, 653 654 3+4+5 (119: 0 >2); (4) well developed posterodorsal expansion of the ischium (131: 0 >1) and 655 (5) horizontal pupil shape (143: 0 >2). Among the Neobatrachia, we recovered a large hyperossified clade, supported by six synapomorphies (see Appendix S4 in Supplemental Data 656 1). Hungarobatrachus is within a poorly supported trichotomy with Eurycephalella and 657 658 Calyptocephalella, for which there are three synapomorphies: (1) contact between lamella 659 alaris of the squamosal and frontoparietals on the dorsal surface of the otic capsule (8: 0 >2); (2) anterior ramus of the pterygoid not reaching planum anteorbitale (12: 0 >1) and (3) 660 postaxial carpal with ulnare and 3 free (119: 2 >1). Cretadhefdaa is recovered within a large 661 662 polytomy with extant Ceratophryidae, poorly supported by four synapomorphies (see Appendix S4 in Supplemental Data 1). 663

This clade is supported by five synapomorphies mainly related to hyperossified cranial

664

665

666

In analyses using a topological constraint (and excluding *Arariphrynus placidoi*), we obtained 190 trees, with a score of 1395 steps. The strict consensus (CI = 0. 126, RI = 0. 247; Fig. 9) shows



a monophyletic Neobatrachia, Ranoides, and Hyloides, but all of the monophyly of each was enforced in the constraint tree. Within Hyloides, most taxa are placed within a large unresolved clade (Fig. 9). *Cretadhefdaa* is recovered in a large polytomy within Hyloides as are *Baurubatrachus*, *Beelzebufo*, *Cratia*, *Eurycephalella*, *Hungarobatrachus*, and *Uberabatrachus*. The only extinct taxon to be recovered elsewhere in the phylogeny is *Thaumastosaurus*, which is recovered in a clade of Ranoides with *Aubria*, *Cornufer*, and *Pyxicephalus*.

Discussion

Phylogenetic analyses

The poor resolution of the topology obtained when performing phylogenetic analysis under equal weights is not surprising. *Hungarobatrachus szukacsi* has only 16 scored characters within the dataset, none of which are clear neobatrachian synapomorphies, and the skeleton of *Arariphrynus* is very incomplete leading to few scored characters, in peculiar regarding pectoral girdle and vertebrae (51 scored characters in total; see Baez et al., 2009). In addition, most of the scored cranial characters for *Hungarobatrachus* and *Cretadhefdaa* are linked to hyperossification, a recurrent feature in anuran evolution (see above) that likely obscures the phylogenetic relationships of *Cretadhefdaa*. One putative synapomorphy of Neobatrachia, the presence of palatine, is inferred in *Cretadhefdaa* (27: 1). When performing the analysis with this character considered as unknown (27: ?), the position of *Cretadhefdaa* does not change (data not shown).



688

689

690

691

692

693

694

695

696

697

698

699

700

701

702

703

704

705

706

707

708

The phylogenetic positions of Cretadhefdaa and Hungarobatrachus are similar to several hyperossified extinct Cretaceous taxa by being close to either the Ceratophryidae or Calyptocephalellidae. Recent analyses (Báez and Gómez, 2018) have highlighted that convergence due to hyperossification likely plays a role in the position recovered for other hyperossified extinct neobatrachian taxa. This could influence the position of Cretadhefdaa as well. Nevertheless, the combination of characters of Cretadhefdaa confirms its assignment to Neobatrachia. In addition, one character mentioned in the description of the braincase, the presence of a series of recesses in posterodorsal region of the braincase, deserves attention. In addition to Cretadhefdaa, a similar (but not clearly homologous) morphology has only been identified in Beelzebufo and in the Ceratophryidae (except in Chacophrys). To our knowledge, this character has not been used in phylogenetic analyses (e.g., Gómez and Turazzini, 2021). However, the two extant taxa possessing these recesses are closely related (Ceratophrys and Lepidobatrachus), and the extinct Beelzebufo has been proposed as a stem member of the Ceratophryidae (Báez and Gómez, 2018; Lemierre et al., 2021). Interestingly, Cretadhefdaa is recovered in a more crownward position within Ceratophryidae than Beelzebufo, even in other analyses (Báez and Gómez, 2018; Lemierre et al., 2021). It is necessary to test the phylogenetic significance of this character to confirm this hypothesis, which is beyond the scope of this paper. When using a topological constraint based on recent phylogenomic analyses, most extinct taxa—including Cretadhefdaa—included in the analysis were recovered as part of Hyloides, though as part of a large polytomy. In conclusion, our phylogenetic analyses point to Cretadhefdaa being within the Neobatrachia, even if most of the synapomorphies diagnostic of this clade are not scored, and several analyses support a hyloid affinity.



710

Paleobiogeographical implications

711 Neobatrachians are known in the fossil record during the Late Cretaceous from three main 712 locations: Madagascar (Maastrichtian; Evans et al., 2014), Europe (Campanian; Venczel et al., 713 2021), and South America (Maastrichtian; Báez and Gómez, 2018). The South American fossil record is of particular importance with numerous taxa known from articulated specimens (Báez 714 et al., 2009; Báez and Gómez, 2018; Agnolin et al., 2020; Moura et al., 2021). In contrast, only 715 fragmentary remains of two taxa have been recovered from Madagascar and Europe (Evans et 716 717 al., 2008; 2014; Venczel et al., 2021). There are other reports of neobatrachians from the 718 Cretaceous (Báez and Werner, 1996; Prasad and Rage, 2004; Rage, 1984; Rage et al., 2020) but 719 the attribution of these to the Neobatrachia remains uncertain because diagnostic elements are often not preserved and these other fossils have not been included in phylogenetic analyses. 720 Because Cretadhefdaa is from the Mid-Cenomanian, it is the oldest neobatrachian of Africa. 721 The oldest occurrence of the Neobatrachia is from the Brazilian Crato Formation (Leal and Brito, 722 723 2006; Báez et al., 2009; Agnolin et al., 2020; Moura et al., 2021), which preserves extinct 724 anurans from the Aptian (Early Cretaceous). However, Cretadhefdaa is still the oldest occurrence of Neobatrachia outside of South America. The Neobatrachia began to diversify 725 726 during the earliest Cretaceous, including an early split into two major lineages, Hyloides and 727 Ranoides, each of which was largely restricted to a portion of western Gondwana, respectively, South America and Africa (Frazão et al., 2015; Feng et al., 2017). Time-calibrated molecular 728 phylogenetic analyses (e.g., Feng et al., 2017) suggest that by 96–95 Ma (i.e., the period from 729





731

732

733

734

735

736

737

738

739

740

741

742

743

744

745

746

747

748

749

750

751

which Cretadhefdaa was recovered), the Neobatrachia was already separated into a number of lineages that are restricted today to specific biogeographic regions. These include the Myobatrachidae of Australia, the hyloids of South America, the Microhylidae (widespread today across the tropics), the Afrobatrachia of sub-Saharan Africa, the natatanuran ranoids, and the lineage leading to the Sooglossidae and Nasikabatrachidae that are today restricted, respectively, to the Seychelles Islands and the Western Ghats of India. There remains ample opportunity for both additional sampling and study of neobatrachian fossils from Gondwanan landmasses that could add new insights into the early evolution and biogeography of these major extant frog lineages that diversified in the Early Cretaceous. The current absence of Ranoides from the Cretaceous fossil record is puzzling. Except for undescribed and unillustrated material that was attributed to Ranoides two decades ago (Báez and Werner, 1996), there is surprisingly few ranoid fossils especially in comparison to the hyloid fossils discovered in South America, Europe, and Africa. Their absence could be due to several factors. The first and most obvious is the lack of anuran specimens from the fossil record of Africa, due both to a lack of targeted collecting and little academic research on existing material. One example that highlights this problem is the Pyxicephalidae, a clade of ranoids endemic to Africa (Channing and Rödel, 2019) and for which time-calibrated molecular phylogenetic analyses suggest a divergence from other natatanurans around 60 Ma (Early Palaeocene). Yet, the oldest occurrence of this family is *Thaumastosaurus* from the Middle-Late Eocene of Europe, whereas the earliest African fossil is from only 5 Ma (Matthews et al., 2015; Lemierre et al., 2021). The large gap in the fossil record of this family is found in many other families of Ranoides, and many clades with an African origin completely lack a fossil record.



Another bias could be that the vast majority of Ranoides are not hyperossified anurans, including many small-sized species, and thus less likely to be preserved as intact and diagnosable fossils. In addition, numerous synapomorphies of Ranoides are for postcranial elements, such as the vertebrae and the pectoral girdle, that are less likely to be identified and/or preserved (Scott, 2005; Frost et al., 2006). A final bias is simply that there has been sustained interest from South American paleontologists in the fossil record of anurans from countries such as Bolivia, Brazil, and Argentina, whereas there have been exceedingly few African paleontologists dedicated to studying anurans.

Conclusion

Our study confirms the report of Rage and Dutheil (2008) that at least three anuran taxa are present in the Kem Kem beds of Morocco. The newly described *Cretadhefdaa taouzensis* can be attributed to the Neobatrachia, making it both the oldest occurrence of the clade outside of South America and only the second occurrence in the Cretaceous of Africa. Several postcranial bones also point to an affinity with the Neobatrachia but cannot be associated definitively with either *Cretadhefdaa* or another taxon. The presence of a neobatrachian in the Kem Kem in the Cenomanian demonstrates that neobatrachians were already widespread on Gondwana during the earliest Late Cretaceous.

Acknowledgement



772	We thank Paul Sereno (University of Chicago) for access to and loan of the specimens, and
773	Edward Stanley (University of Florida) for CT-scanning them. Processing of tomographic data
774	was undertaken at the 3D imaging facilities Lab of the UMR 7207 CR2P (MNHN CNRS UPMC,
775	Paris). We thank María Vallejo-Pareja for comments on a draft of this manuscript.
776	
777	References
778	Agnolin F. 2012. A New Calyptocephalellidae (anura, Neobatrachia) from the Upper Cretaceous
779	of Patagonia, Argentina, with Comments on Its Systematic Position. Studia Geologica
780	Salmanticensia 48:129–178.
781	Agnolin F, Carvalho I de S, Aranciaga Rolando AM, Novas FE, Xavier-Neto J, Andrade JAFG,
782	Freitas FI. 2020. Early Cretaceous neobatrachian frog (Anura) from Brazil sheds light on the
783	origin of modern anurans. Journal of South American Earth Sciences 101:102633. DOI:
784	10.1016/j.jsames.2020.102633.
785	Báez AM, Gómez RO. 2018. Dealing with homoplasy: osteology and phylogenetic relationships
786	of the bizarre neobatrachian frog Baurubatrachus pricei from the Upper Cretaceous of Brazil.
787	Journal of Systematic Palaeontology 16:279–308. DOI: <u>10.1080/14772019.2017.1287130</u> .
788	Báez AM, Gómez RO, Ribeiro LCB, Martinelli AG, Teixeira VPA, Ferraz MLF. 2012. The diverse
789	Cretaceous neobatrachian fauna of South America: Uberabatrachus carvalhoi, a new frog from
790	the Maastrichtian Marília Formation, Minas Gerais, Brazil. <i>Gondwana Research</i> 22:1141–1150.
791	DOI: <u>10.1016/j.gr.2012.02.021</u> .



- 792 Báez AM, Moura GJB, Gómez RO. 2009. Anurans from the Lower Cretaceous Crato Formation of
- 793 northeastern Brazil: implications for the early divergence of neobatrachians. *Cretaceous*
- 794 *Research* 30:829–846. DOI: 10.1016/j.cretres.2009.01.002.
- 795 Báez AM, Perí S. 1989. Baurubatrachus pricei, nov. gen. et sp., un Anuro del Cretacico Superior
- 796 de Minas Gerais. Anais da Academia Brasileira de Ciências 61:447–458.
- 797 Báez AM, Rage J-C. 1998. Pipid frogs from the Upper Cretaceous of In Beceten, Niger.
- 798 *Palaeontology* 41:669–691.
- 799 Báez AM, Werner C. 1996. Presencia de Anuros Ranoideos en el Cretácico de Sudan.
- 800 AMEGHINIANA 33:460.
- 801 Biton R, Boistel R, Rabinovich R, Gafny S, Brumfeld V, Bailon S. 2016. Osteological observations
- 802 on the Alytid Anura Latonia nigriventer with comments on functional morphology,
- 803 biogeography, and evolutionary history. *Journal of Morphology* 277:1131–1145. DOI:
- 804 10.1002/jmor.20562.
- 805 Blakey RC. 2008. Gondwana paleobiogeography from assembly to breakup—A 500 m.y.
- 806 odyssey. In: Fielding CR, Frank TD, Isbell JL eds. Resolving the Late Paleozoic Ice Age in time and
- 807 space. The Geological Society of America Special Paper. Boulder, CO, USA: The Geological
- 808 Society of America, 1–28.
- 809 de Broin F, Buffetaut E, Koeniger J-C, Rage J, Russell D, Taquet P, Vergnaud-Grazzini C, Wenz S.
- 810 1974. La faune de vertébrés continentaux du gisement d'In Betceten (Sénonien du Niger).
- 811 Comptes Rendus de l'Académie des Sciences, Paris 279:439–472.





821

822

823

824

813	G, Hua S, Le Loeuff J. 2010. Vertebrate assemblages from the early Late Cretaceous of
814	southeastern Morocco: An overview. <i>Journal of African Earth Sciences</i> 57:391–412. DOI:
815	10.1016/j.jafrearsci.2009.12.007.
816	Channing A, Rödel M-O. 2019. Field Guide to the Frogs & Other Amphibians of Africa. Penguin
817	Random House South Africa.
818	Duellman WE, Trueb L. 1994. Biology of Amphibians. JHU Press.
819	Dutheil DB. 1999. An overview of the freshwater fish fauna from the Kem Kem beds (Late
820	Cretaceous: Cenomanian) of southesatern Morocco. In: Arrratia G, Schultze HP eds. <i>Mesozoic</i>

fishes-Systematics and fossil record. Munich: F. Pfeil, 553-563.

Cavin L, Tong H, Boudad L, Meister C, Piuz A, Tabouelle J, Aarab M, Amiot R, Buffetaut E, Dyke

Ettachfini EM, Andreu B. 2004. Le Cénomanien et le Turonien de la Plate-forme Préafricaine du

Evans SE, Groenke JR, Jones MEH, Turner AH, Krause DW. 2014. New Material of Beelzebufo, a

Maroc. *Cretaceous Research* 25:277–302. DOI: <u>10.1016/j.cretres.2004.01.001</u>.



- Fabrezi M. 2006. Morphological evolution of Ceratophryinae (Anura, Neobatrachia). *Journal of*
- Zoological Systematics and Evolutionary Research 44:153–166. DOI: 10.1111/j.1439-
- 832 0469.2005.00349.x.
- Feng Y-J, Blackburn DC, Liang D, Hillis DM, Wake DB, Cannatella DC, Zhang P. 2017.
- 834 Phylogenomics reveals rapid, simultaneous diversification of three major clades of Gondwanan
- 835 frogs at the Cretaceous–Paleogene boundary. *Proceedings of the National Academy of Sciences*
- 836 114:E5864–E5870. DOI: <u>10.1073/pnas.1704632114</u>.
- 837 Filhol H. 1877. Recherches sur les phosphorites du Quercy: Etude des fossiles qu'on y rencontre
- 838 et spécialement des mammifères. Paris.
- 839 Frazão A, Silva HR da, Russo CA de M. 2015. The Gondwana Breakup and the History of the
- 840 Atlantic and Indian Oceans Unveils Two New Clades for Early Neobatrachian Diversification.
- 841 *PLOS ONE* 10:e0143926. DOI: <u>10.1371/journal.pone.0143926</u>.
- 842 Frishkopf LS, Goldstein MH. 1963. Responses to Acoustic Stimuli from Single Units in the Eighth
- 843 Nerve of the Bullfrog. *The Journal of the Acoustical Society of America* 35:1219–1228. DOI:
- 844 10.1121/1.1918676.
- 845 Frost DR, Grant T, Faivovich J, Bain RH, Haas A, Haddad CFB, De Sá RO, Channing A, Wilkinson
- 846 M, Donnellan SC, Raxworthy CJ, Campbell JA, Blotto BL, Moler P, Drewes RC, Nussbaum RA,
- Lynch JD, Green DM, Wheeler WC. 2006. The Amphibian Tree of Life. Bulletin of the American
- 848 *Museum of Natural History* 297:1–291. DOI: 10.1206/0003-
- 849 <u>0090(2006)297[0001:TATOL]2.0.CO;2.</u>





850	Gardner JD, Rage J-C. 2016. The fossil record of lissamphibians from Africa, Madagascar, and
851	the Arabian Plate. Palaeobiodiversity and Palaeoenvironments 96:169–220. DOI:
852	10.1007/s12549-015-0221-0.
853	Gardner JD, Roček Z, Přikryl T, Eaton JG, Blob RW, Sankey JT. 2010. Comparative morphology of
854	the ilium of anurans and urodeles (Lissamphibia) and a re-assessment of the anuran affinities of
855	Nezpercius dodsoni Blob et al., 2001. Journal of Vertebrate Paleontology 30:1684–1696. DOI:
856	<u>10.1080/02724634.2010.521605</u> .
857	Gaupp E. 1896. Anatomie des Frosches. Pt. 3. Braunschweg: Friedrich Vieweg Und Shon.
858	Goloboff PA, Catalano SA. 2016. TNT version 1.5, including a full implementation of
859	phylogenetic morphometrics. <i>Cladistics</i> 32:221–238. DOI: <u>10.1111/cla.12160</u> .
860	Gómez RO, Turazzini GF. 2016. An overview of the ilium of anurans (Lissamphibia, Salientia),
861	with a critical appraisal of the terminology and primary homology of main ilial features. Journal
862	of Vertebrate Paleontology 36:e1030023. DOI: <u>10.1080/02724634.2015.1030023</u> .
863	Gómez RO, Turazzini GF. 2021. The fossil record and phylogeny of South American horned frogs
864	(Anura, Ceratophryidae). Journal of Systematic Palaeontology 0:1–52. DOI:
865	10.1080/14772019.2021.1892845.
866	Hime PM, Lemmon AR, Lemmon ECM, Prendini E, Brown JM, Thomson RC, Kratovil JD, Noonan
867	BP, Pyron RA, Peloso PLV, Kortyna ML, Keogh JS, Donnellan SC, Mueller RL, Raxworthy CJ, Kunte
868	K, Ron SR, Das S, Gaitonde N, Green DM, Labisko J, Che J, Weisrock DW. 2021. Phylogenomics



869	Reveals Ancient Gene Tree Discordance in the Amphibian Tree of Life. Systematic Biology
870	70:49–66. DOI: <u>10.1093/sysbio/syaa034</u> .
871	Ibrahim N, Sereno PC, Varricchio DJ, Martill DM, Dutheil DB, Unwin DM, Baidder L, Larsson HCE
872	Zouhri S, Kaoukaya A. 2020. Geology and paleontology of the Upper Cretaceous Kem Kem
873	Group of eastern Morocco. <i>ZooKeys</i> 928:1–216. DOI: <u>10.3897/zookeys.928.47517</u> .
874	Jacobs LL, Winkler DA, Gomani EM. 1990. The Dinosaur Beds of northern Malawi, Africa.
875	National Geographic Research 6:196–204.
876	Jetz W, Pyron RA. 2018. The interplay of past diversification and evolutionary isolation with
877	present imperilment across the amphibian tree of life. <i>Nature Ecology & Evolution</i> 2:850–858.
878	DOI: <u>10.1038/s41559-018-0515-5</u> .
879	de Lapparent de Broin F, Bailon S, Augé ML, Rage J-C. 2020. Amphibians and reptiles from the
880	Neogene of Afghanistan. <i>Geodiversitas</i> 42:409–426.
881	Leal MEC, Brito PM. 2006. Anura do Cretáceo Inferior da Bacia do Araripe, Nordeste do Brasil.
882	In: Gallo V, Brito PM, Silva HMA, Figueiredo FJ eds. Paleontología de Vertebrados. Grandes
883	Temas e Contribuçoes Científicas. Rio de Janeiro: Interciencia, 145–152.
884	Lemierre A, Folie A, Bailon S, Robin N, Laurin M. 2021. From toad to frog, a CT-based
885	reconsideration of Bufo servatus, an Eocene anuran mummy from Quercy (France). Journal of
886	Vertebrate Paleontology 41:e1989694. DOI: <u>10.1080/02724634.2021.1989694</u> .
887	Maddin HC, Venczel M, Gardner JD, Rage J-C. 2013. Micro-computed tomography study of a
888	three-dimensionally preserved neurocranium of Albanerpeton (Lissamphibia,





889	Albanerpetontidae) from the Pliocene of Hungary. Journal of Vertebrate Paleontology 33:568–
890	587. DOI: <u>10.1080/02724634.2013.722899</u> .
891	Matthews T, van Dijk E, Roberts DL, Smith RMH. 2015. An early Pliocene (5.1 Ma) fossil frog
892	community from Langebaanweg, south-western Cape, South Africa. African Journal of
893	Herpetology 64:39–53. DOI: <u>10.1080/21564574.2014.985261</u> .
894	Matthews T, Keeffe R, Blackburn DC. 2019. An identification guide to fossil frog assemblages of
895	southern Africa based on ilia of extant taxa. Zoologischer Anzeiger 283:46–57. DOI:
896	10.1016/j.jcz.2019.08.005.
897	McLoughlin S. 2001. The breakup history of Gondwana and its impact on pre-Cenozoic floristic
898	provincialism. <i>Australian Journal of Botany</i> 49:271. DOI: <u>10.1071/BT00023</u> .
899	Moura PHAG, Costa FR, Anelli LE, Nunes I. 2021. A new genus of fossil frog (Anura) from lower
900	Cretaceous deposits in South America. <i>Anais da Academia Brasileira de Ciências</i> 93:e20191560.
901	DOI: <u>10.1590/0001-3765202120201560</u> .
902	Muzzopappa P, Báez AM. 2009. Systematic status of the mid-Tertiary neobatrachian frog
903	Calyptocephalella canqueli from Patagonia (Argentina), with comments on the evolution of the
904	genus. AMEGHINIANA 46:113–125.
905	Muzzopappa P, Martinelli AG, Garderes JP, Rougier GW. 2020. Exceptional avian pellet from the
906	Paleocene of Patagonia and description of its content: a new species of calyptocephalellid
907	(Neobatrachia) anuran. <i>Papers in Palaeontology</i> :spp2.1333. DOI: <u>10.1002/spp2.1333</u> .



9@aluh DJ, Stanley EL, Blackburn DC. 2020. Evolution of hyperossification expands skull diversity in

- 909 frogs. Proceedings of the National Academy of Sciences 117:8554–8562. DOI:
- 910 <u>10.1073/pnas.2000872117</u>.
- 911 Prasad GVR, Rage J-C. 2004. Fossil frogs (Amphibia: Anura) from the Upper Cretaceous
- 912 intertrappean beds of Naskal, Andhra Pradesh, India. Revue de Paléobiologie, Genève 23:99-
- 913 116.
- Rage J-C. 1984. Are the Ranidae (Anura, Amphibia) known prior to the Oligocene? *Amphibia*-
- 915 Reptilia 5:281–288. DOI: 10.1163/156853884X-005-03-09.
- 916 Rage J-C. 2008. Amphibia (Anura) from the Lower Miocene of the Sperrgebiet, Namibia. Memoir
- 917 of the Geological Survey of Namibia 20:75–92.
- 918 Rage J-C, Adaci M, Bensalah M, Mahboubi M, Marivaux L, Mebrouk F, Tabuce R. 2021. Lastest
- 919 Early-Middle Eocene deposits of Algeria (Glib Zegdou, HGL50) yield the richest and most diverse
- 920 fauna of amphibians and squamate reptiles from the Palaeogene of Africa. Paleovertebrata 43.
- 921 Rage J-C, Dutheil DB. 2008. Amphibians and squamates from the Cretaceous (Cenomanian) of
- 922 Morocco A preliminary study, with description of a new genus of pipid frog.
- 923 Palaeontographica Abteilung A 285:1–22. DOI: 10.1127/pala/285/2008/1.
- 924 Rage J-C, Pickford M, Senut B. 2013. Amphibians and squamates from the middle Eocene of
- Namibia, with comments on pre-Miocene anurans from Africa. *Annales de Paléontologie*
- 926 99:217–242. DOI: 10.1016/j.annpal.2013.04.001.



927	Rage J-C, Prasad GVR, Verma O, Khosla A, Parmar V. 2020. Anuran Lissamphibian and Squamate
928	Reptiles from the Upper Cretaceous (Maastrichtian) Deccan Intertrappean Sites in Central India,
929	with a Review of Lissamphibian and Squamate Diversity in the Northward Drifting Indian Plate.
930	In: Prasad GVR, Patnaik R eds. Biological Consequences of Plate Tectonics. Vertebrate
931	Paleobiology and Paleoanthropology. Cham: Springer International Publishing, 99–121. DOI:
932	<u>10.1007/978-3-030-49753-8_6</u> .
933	Rage J-C, Roček Z. 2003. Evolution of anuran assemblages in the Tertiary and Quaternary of
934	Europe, in the context of palaeoclimate and palaeogeography. <i>Amphibia-Reptilia</i> 24:133–167.
935	DOI: <u>10.1163/156853803322390408</u> .
936	Rage J, Roček Z. 2007. A new species of <i>Thaumastosaurus</i> (Amphibia: Anura) from the Eocene
937	of Europe. Journal of Vertebrate Paleontology 27:329–336. DOI: 10.1671/0272-
938	4634(2007)27[329:ANSOTA]2.0.CO;2.
939	Rineau V, i Bagils RZ, Laurin M. 2018. Impact of errors on cladistic inference: simulation-based
940	comparison between parsimony and three-taxon analysis. Contributions to Zoology 87:25–40.
941	DOI: <u>10.1163/18759866-08701003</u> .
942	Rineau V, Grand A, Zaragüeta R, Laurin M. 2015. Experimental systematics: sensitivity of
943	cladistic methods to polarization and character ordering schemes. Contributions to Zoology
944	84:129–148. DOI: <u>10.1163/18759866-08402003</u> .
945	Roček Z. 1994. Taxonomy and Distribution of Tertiary Discoglossids (anura) of The Genus
946	Latonia V. Meyer, 1843. <i>Geobios</i> 27:717–751.





947	Rocek Z. 2000. Mesozoic Anurans. In: Heatwole H, Carroll RL eds. <i>Palaeontology The</i>
948	Evolutionnary History of Amphibians. Amphibian Blology. 1295–1331.
949	Roček Z. 2008. The Late Cretaceous frog Gobiates from Central Asia: its evolutionary status and
950	possible phylogenetic relationships. <i>Cretaceous Research</i> 29:577–591. DOI:
951	<u>10.1016/j.cretres.2008.01.005</u> .
952	Roček Z. 2013. Mesozoic and Tertiary Anura of Laurasia. Palaeobiodiversity and
953	<i>Palaeoenvironments</i> 93:397–439. DOI: <u>10.1007/s12549-013-0131-y</u> .
954	Roček Z, Eaton JG, Gardner JD, Přikryl T. 2010. Evolution of anuran assemblages in the Late
955	Cretaceous of Utah, USA. Palaeobiodiversity and Palaeoenvironments 90:341–393.
956	Roček Z, Wuttke M, Gardner JD, Singh Bhullar B-A. 2014. The Euro-American genus
957	Eopelobates, and a re-definition of the family Pelobatidae (Amphibia, Anura). Palaeobiodiversit
958	and Palaeoenvironments 94:529–567. DOI: <u>10.1007/s12549-014-0169-5</u> .
959	Roelants K, Gower DJ, Wilkinson M, Loader SP, Biju SD, Guillaume K, Moriau L, Bossuyt F. 2007.
960	Global patterns of diversification in the history of modern amphibians. Proceedings of the
961	National Academy of Sciences 104:887–892. DOI: <u>10.1073/pnas.0608378104</u> .
962	Scott E. 2005. A phylogeny of ranid frogs (Anura: Ranoidea: Ranidae), based on a simultaneous
963	analysis of morphological and molecular data. <i>Cladistics</i> 21:507–574. DOI: <u>10.1111/j.1096-</u>
964	0031.2005.00079.x.



965	Sereno PC, Dutheil DB, Iarochene M, Larsson HCE, Lyon GH, Magwene PM, Sidor CA, Varricchio
966	DJ, Wilson JA. 1996. Predatory Dinosaurs from the Sahara and Late Cretaceous Faunal
967	Differentiation. <i>Science</i> 272:986–991. DOI: <u>10.1126/science.272.5264.986</u> .
968	Streicher, J.W., Miller, E.C., Guerrero, P.C., Correa, C., Ortiz, J.C., Crawford, A.J., Pie, M.R. and
969	Wiens, J.J., 2018. Evaluating methods for phylogenomic analyses, and a new phylogeny for a
970	major frog clade (Hyloidea) based on 2214 loci. Molecular Phylogenetics and Evolution,
971	119:128-143.
972	Szentesi Z, Venczel M. 2010. An advanced anuran from the Late Cretaceous (Santonian) of
973	Hungary. Neues Jahrbuch für Geologie und Paläontologie - Abhandlungen 256:291–302. DOI:
974	10.1127/0077-7749/2010/0054.
975	Trueb L. 1973. Bones, Frogs and Evolution. In: Vial JL ed. Evolutionary Biology of the Anurans.
976	Contemporary Research on Major Problems. Columbia: University of Missouri Press, 65–133.
977	Trueb L, Púgener LA, Maglia AM. 2000. Ontogeny of the bizarre: an osteological description of
978	Pipa pipa (Anura: Pipidae), with an account of skeletal development in the species. Journal of
979	Morphology 243:75–104. DOI: <u>10.1002/(SICI)1097-4687(200001)243:1<75::AID-</u>
980	JMOR4>3.0.CO;2-L.
981	Venczel M, Szentesi Z, Gardner JD. 2021. New material of the frog <i>Hungarobatrachus szukacsi</i>
982	Szentesi & Venczel, 2010, from the Santonian of Hungary, supports its neobatrachian affinities
983	and reveals a Gondwanan influence on the European Late Cretaceous anuran fauna.
984	Geodiversitas 43. DOI: 10.5252/geodiversitas2021v43a7.



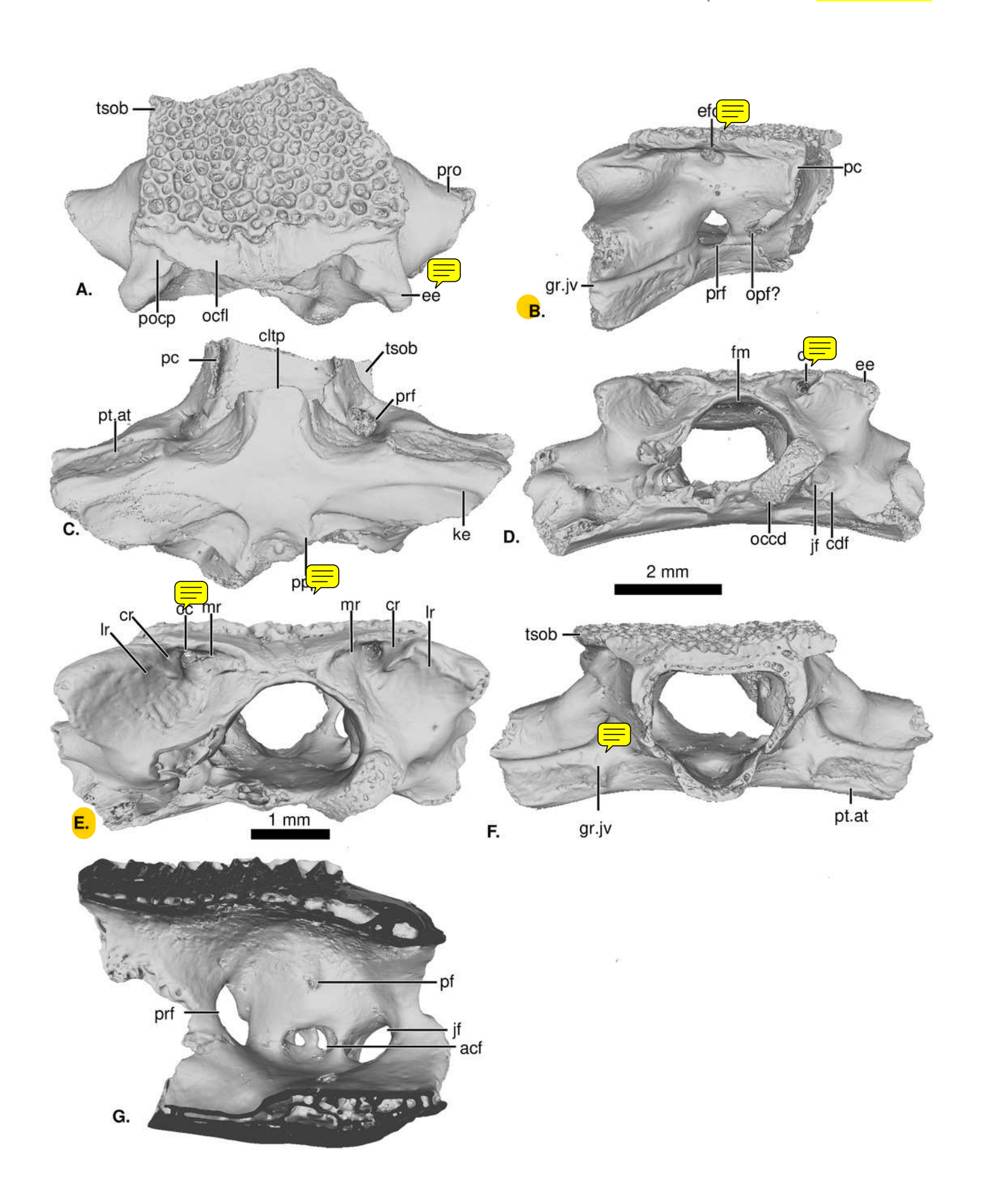


985	Wever EG. 1979. Middle ear muscles of the frog. Proceedings of the National Academy of
986	Sciences 76:3031–3033. DOI: <u>10.1073/pnas.76.6.3031</u> .
987	Wever EG. 1985. <i>The Amphibian Ear</i> . Princeton, New Jeresy, USA: Princeton University Press.
988	Yuan, Z.Y., Zhang, B.L., Raxworthy, C.J., Weisrock, D.W., Hime, P.M., Jin, J.Q., Lemmon, E.M.,
989	Lemmon, A.R., Holland, S.D., Kortyna, M.L. and Zhou, W.W., 2018. Natatanuran frogs used the
990	Indian Plate to step-stone disperse and radiate across the Indian Ocean. National Science
991	Review, 6:10-14.
992	Zouhri S (ed.). 2017. Paléontologie des vertébrés du Maroc: état des connaissances. Paris.



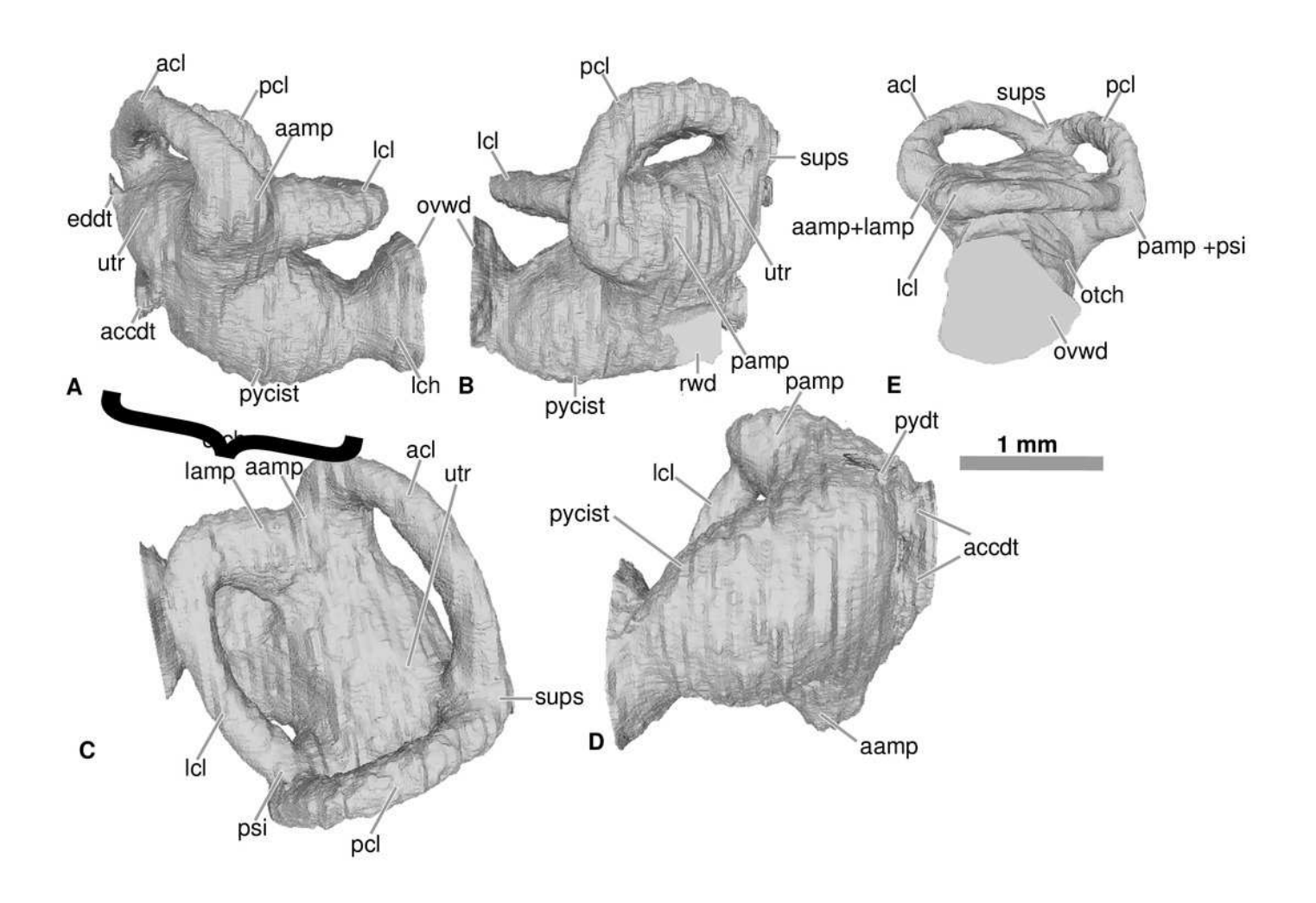
UCRC-PV64, holotype of Cretadhefdaa

Incomplete braincase in **A** dorsal; **B** ventral; **C** anterior; **D** posterior; **E** left lateral; and **F** left medial views. Same specimen in **G** posterodorsal view with a close up on the recesses system. **Abbreviations**: **acf?**, fused acoustic foramina; **cc**, carotid canal; **cdf**, condyloid fossa; **cltp**, cultriform process; **cr?**, central recess; **ee**, epiotic eminence; **efca**, exit foramen for the carotic rtera; **fm**, foramen magnum; **gr.jv**, groove for the jugular vein; **jf**, jugular foramen; **ke**, median keel; **Ir**, lateral recess; **mr**, medial recess; **occd**, occipital condyle; **opt?**, optical foramen; **pc**, pars contacta; **pf**, perilymphatic foramen; **pocp**, paraoccipital process; **ppp**, posterior process of the parasphenoid; **prf**, prootic foramen; **pro**, prootic, **pt.at**, pterygoid attachment area; **tsob**, tectum supraorbitale.



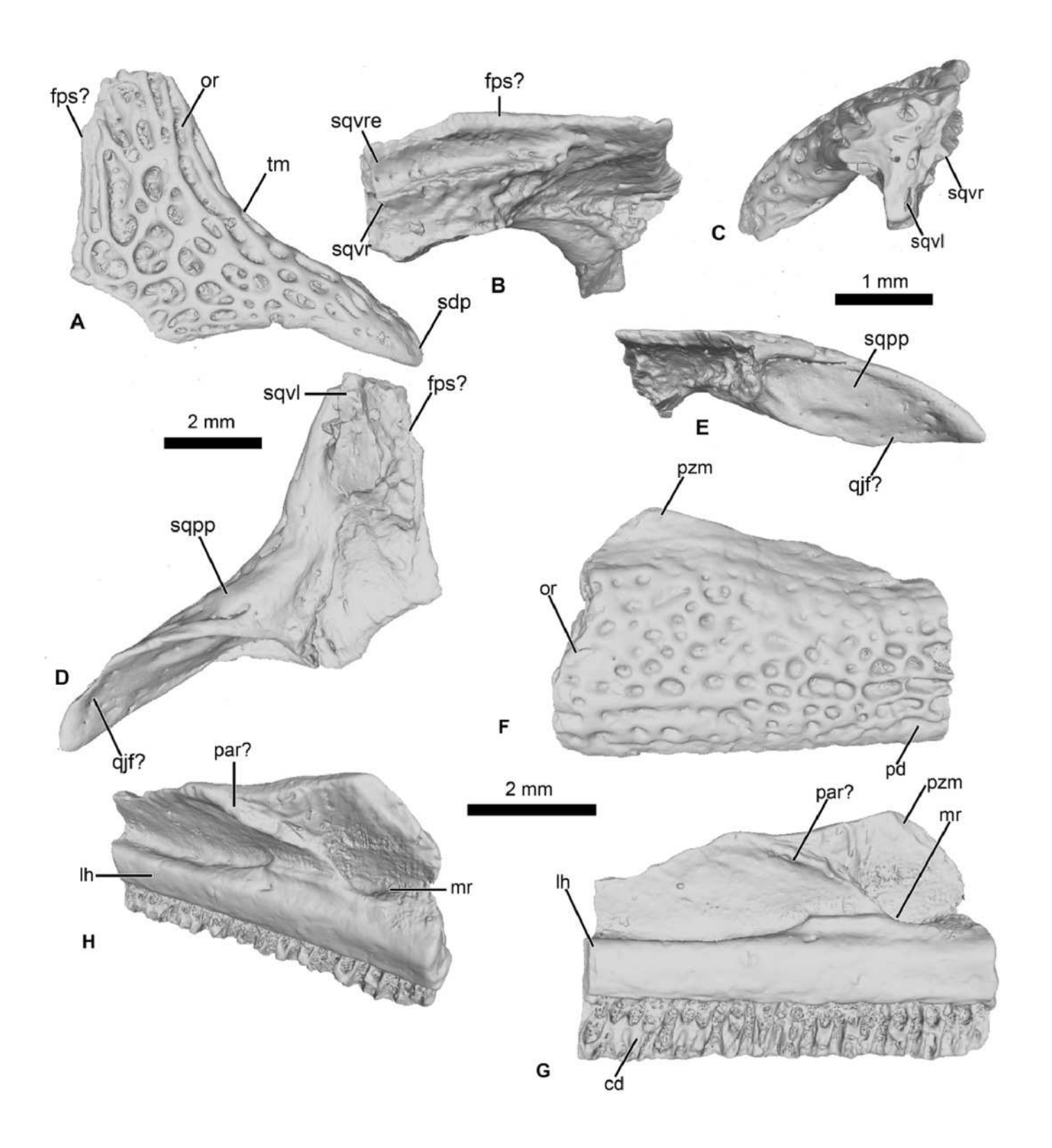
Interior morphology of the otic capsule of *Cretadhefdaa*

Inner ear in **A** anterior; **B** posterior; **C** dorsal; **D** ventral and **E** lateral views. **Abbreviations**: **aamp**, anterior ampulla; **accdt**, acoustic duct; **acl**, anterior canal; **eddt**, endolymphatic duct; **lamp**, lateral ampulla; **lch**, lateral chamber; **lcl**, lateral canal; **otch**, otic chamber; **ovw**, oval window; **pamp**, posterior ampulla; **pcl**, posterior canal; **psi**, posterior sinus; **pycist**, perilymphatic cistern; **pydt**, perilymphatic duct; **rwd**, round window; **sups**, superior sinus; **utr**, utricle.



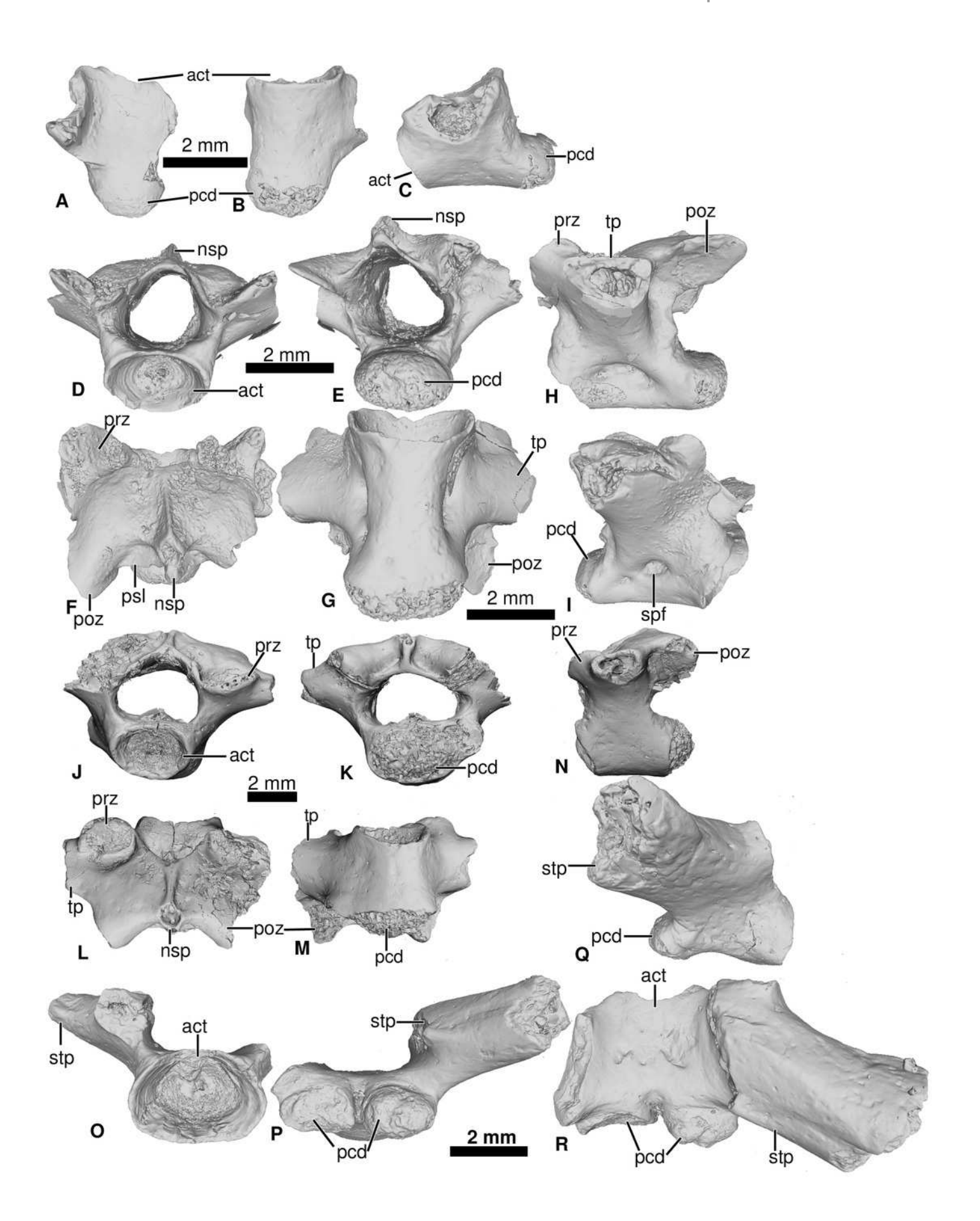
Cranial elements of Cretadhefdaa

A - E UCRC-PV95, incomplete squamosal in A, dorsal; B medial; C anterior; D posterior and E ventral views; F-G UCRC-PV94, incomplete xilla in F lateral, G medial and H dorsomedial views. Abbreviations: cd, crista dentalis; fps?, frontoparietal suture ?; Ih, lamina horizontalis; mr, medial ridge; or, ornamentation; par?; palatine articulation; pzm, processus zygomatico-maxillaris; qjf?; quadratojugal facet ?; sqvI, squamosal ventral lamina; sqvr, squamosal ventral ridge; squvre, squamosal ventral recess; tm, temporal margin.



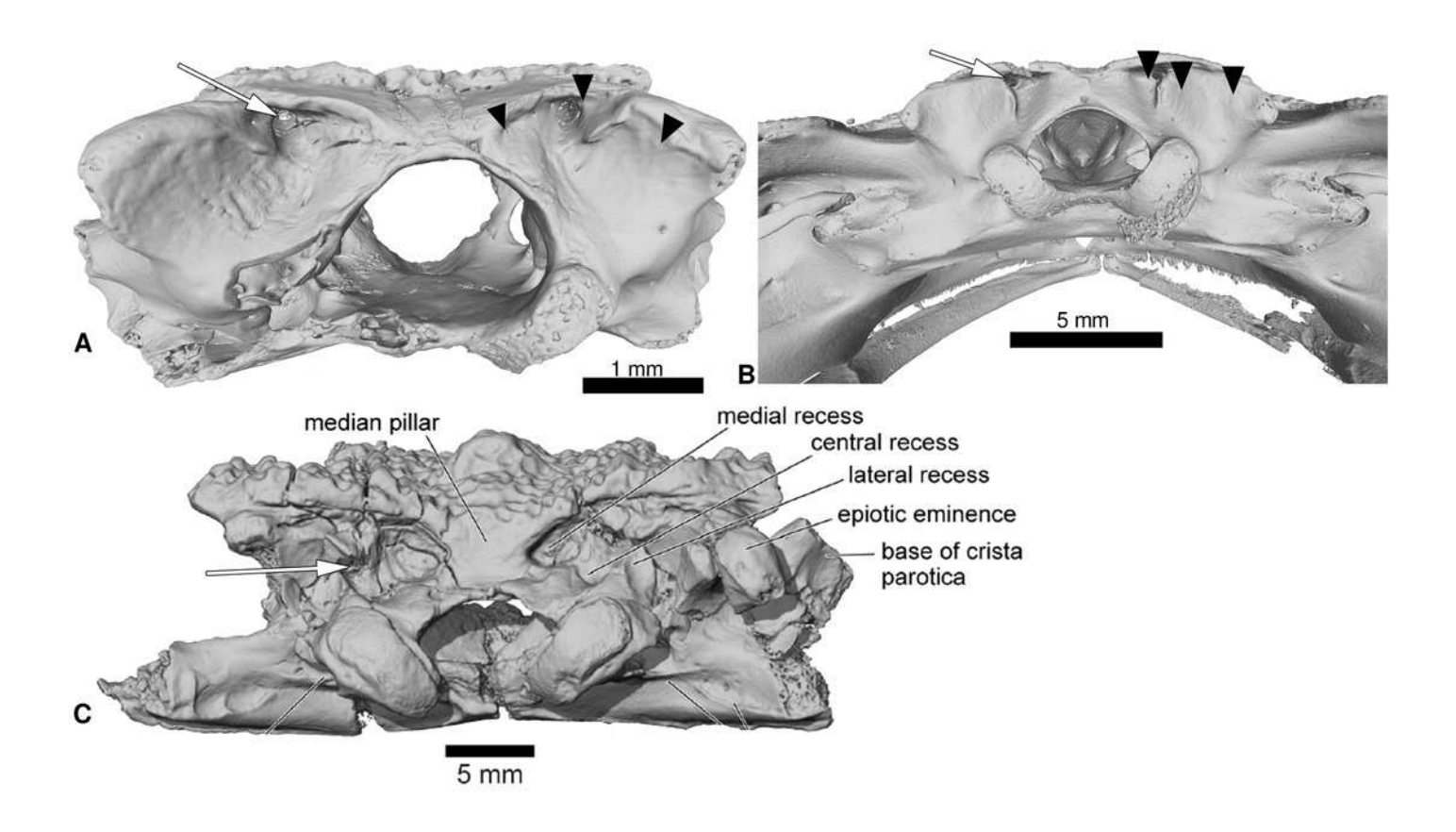
Vertebral element of Cretadhefdaa

A-C UCRC-PV97, presacral centrum in A dorsal; B ventral and C right lateral views; D-I UCRC-PV98 incomplete possible presacral vertebra IV in D anterior; E posterior; F dorsal; G ventral; H left lateral and I right lateral views; J-N UCRC-PV101, incomplete possible presacral VIII in J anterior; K posterior; L dorsal; M ventral and N left lateral views; O-R UCRC-PV103, incomplete sacral vertebra in O anterior; P posterior; Q right lateral and R ventral views. Abbreviations: act, anterior cotyle; nsp, neural spine; pcd, posterior condyle; poz, postzygapophyse; prz, prezygapophyse; psl, posterior lamina; spf, spinal foramen; stp, sacral transverse process; tp, transverse process.



Comparison between the braincases of Cretadhefdaa, Beelzebufo and Ceratophryidae

A *Cretadhefdaa* in posterior view (UCRC-PV64); **B** *Beelzebufo* braincase in posterior view (taken from Evans et al., 2014: fig. 22C) and **C** braincase of *Ceratophrys aurita* in posterior view (CAS:Herp:84998; MorphoSource ARK: ark:/87602/m4/M16099). Black arrows point to the recesses discussed in the text

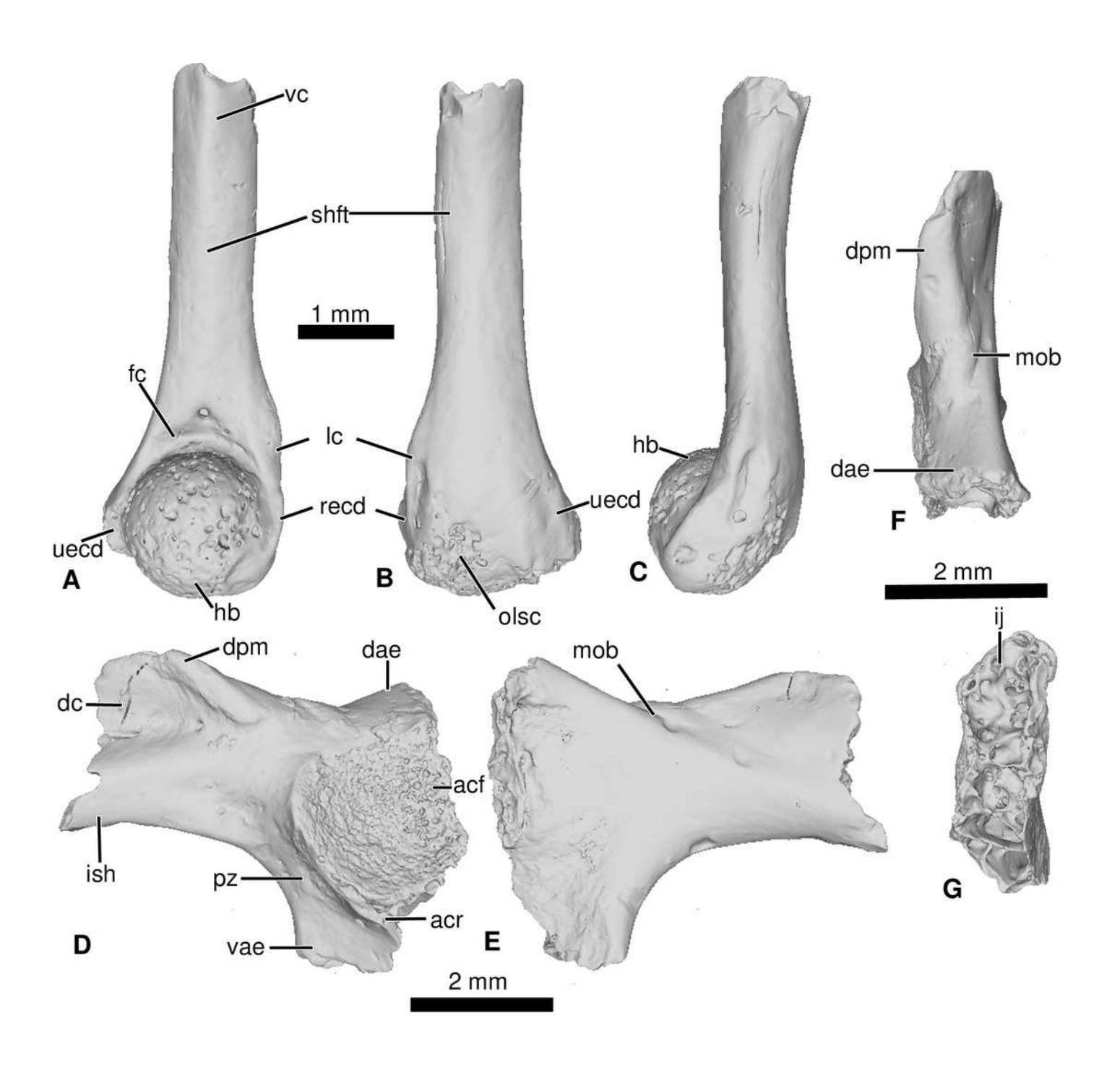




Neobatrachia? and indeterminate ilium from Kem Kem beds

A-C, UCRC-PV104, incomplete humerus in A ventral; B dorsal and C lateral views; D-G, UCRC-PV105, left ilium in D lateral; E medial; F posterior and G dorsal views.

Abbreviations: acf, acetabular fossa; acr, acetabular rim; dae, dorsal acetabular expansion; dc, dorsal crest; dpm, dorsal prominence; fc, fossa cubitalis; hb, humeral ball; ij, ilioischiatic juncture; ish, iliac shaft; lc, lateral crest; mob, medial oblique ridge; olsc; olecranon scar; pz, preacetabular zone; recd, radial (lateral) epicondyle; shft, shaft; uecd, ulnare (medial) epicondyle; vae, ventral acetabular expansion; vc, ventral crest.

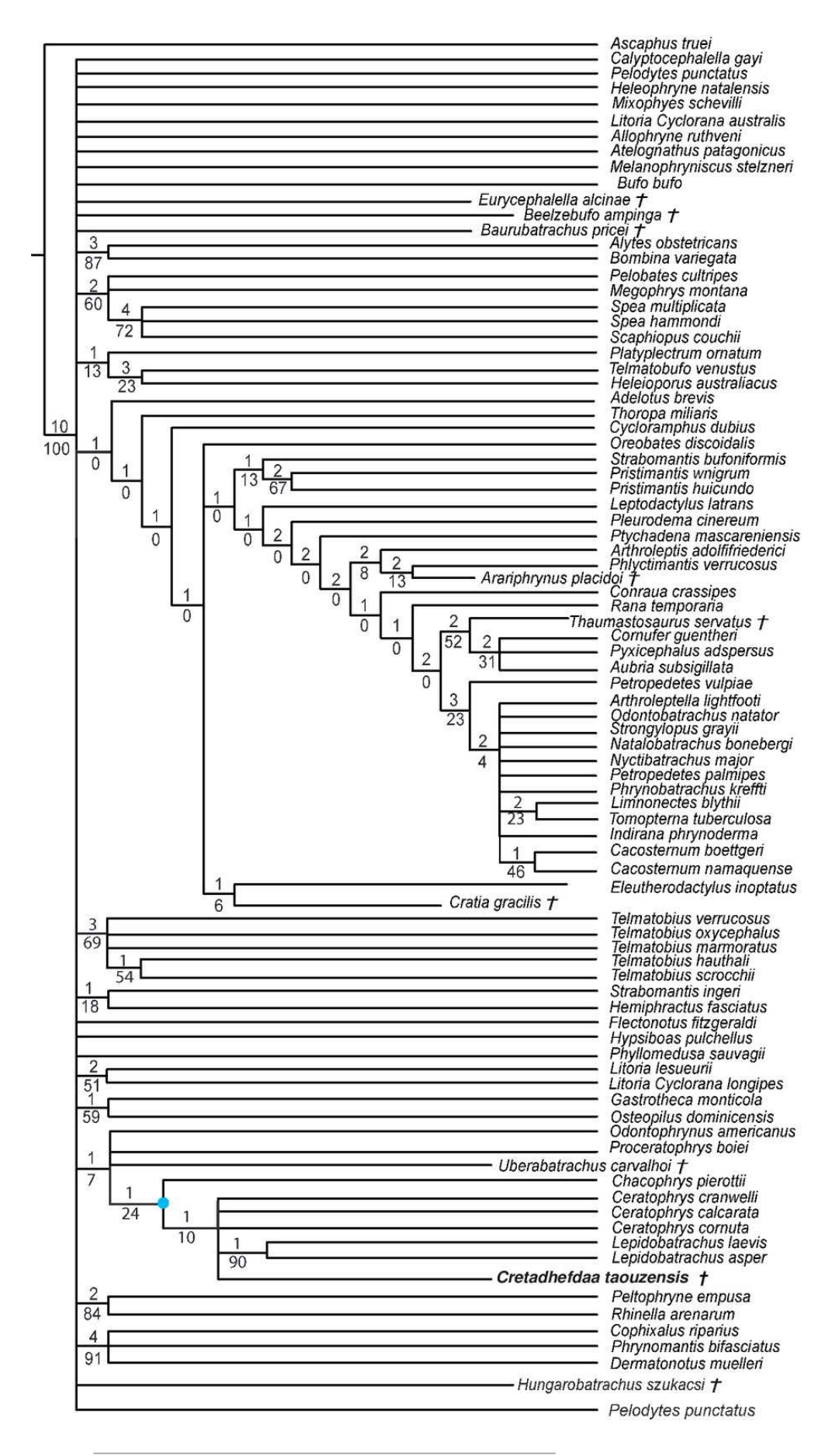




Strict consensus of 60 MPTs of 1362 steps (CI = 0.139; RI = 0.418) from the analysis under EW

† represents extinct taxon, red circle represents Neobatrachia node (excluding *Heleophryne*), light blue circle represents Ceratophryidae node.



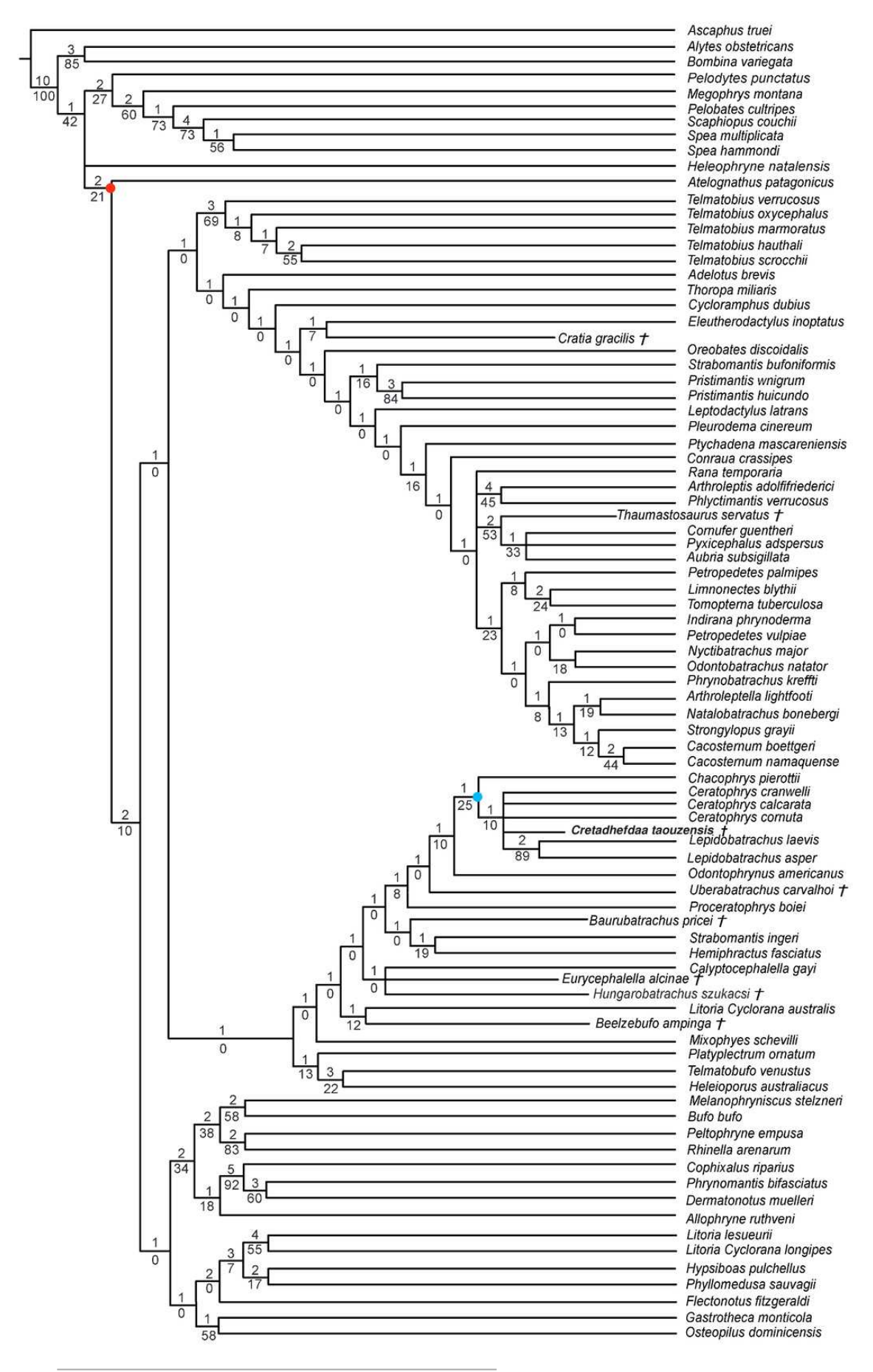




Strict consensus of 10 MPTs of 1355 steps (CI = 0.174; RI = 0.556) from the analysis under EW excluding *Arariphrynus placidoi*

† represents extinct taxon, red circle represents Neobatrachia node (excluding *Heleophryne*), and light blue circle represents Ceratophryidae node.







Strict consensus of 190 MPTs of 1395 steps (CI = 0.126; RI = 0.247) from the analysis under EW, excluding *Arariphrynus placidoi* and using a constraint topology based on molecular phylogenetic analyses

† represents extinct taxon.



